SUPPORTING INFORMATION for:

Triazolyl-Based Copper-Molybdate Hybrids: From Composition-Space Diagram to Magnetism and Catalytic Performance

Ganna A. Senchyk,[a] Andrey B. Lysenko,[a] Artem A. Babaryk,[a] Eduard B. Rusanov,[b] Harald Krautscheid,[c] Patrícia Neves,[d] Anabela A. Valente,[d] Isabel S. Gonçalves,[d] Karl W. Krämer,[e] Shi-Xia Liu,[e*] Silvio Decurtins,[e] Konstantin V. Domasevitch[a]*

[a] *Inorganic Chemistry Department, Taras Shevchenko National University of Kyiv, Volodimirska Str. 64, Kyiv 01033, Ukraine*

[b] *Institute of Organic Chemistry, Murmanska Str. 5, Kyiv, 02660, Ukraine*

[c] *Institut für Anorganische Chemie, Universität Leipzig, Johannisallee 29, D-04103 Leipzig, Germany*

[d] *Department of Chemistry, CICECO, University of Aveiro, Campus Universitário de Santiago, 3810-193 Aveiro, Portugal*

[e] *Departement für Chemie und Biochemie, Universität Bern, Freiestrasse 3, CH-3012 Bern, Switzerland*

- Corresponding author. E-mail address: ab_lysenko@univ.kiev.ua (Lysenko A.B.)

X-ray Crystallography

The diffraction data were collected with graphite-monochromated Mo Kα radiation (λ = 0.71073 Å). Measurements for **1** at 213 K and for **2** and **4** at 296 K were performed K on a Bruker APEXII CCD area-detector diffractometer (ω scans). The data were corrected for Lorentz-polarization effects and for the effects of absorption (multi-scans method). Measurements for **3** at 213 K were made using a Stoe Image Plate Diffraction System, φ oscillation scans (numerical absorption correction using X-RED and X-SHAPE).[S1] The structures were solved by direct methods and refined by full-matrix least-squares on F^2 using the SHELX-97 package.[S2] Graphical visualization of the structures was made using the program Diamond 2.1e.[S3]

Refinement of (1).

The refinement was essentially standard. Due to a relatively weak diffraction pattern collected for the small crystal (0.02 × 0.10 × 0.10 mm), a resolution limit of 0.82 Å was applied to the data. The CH-hydrogen atoms were added geometrically and refined as riding, with U_{iso} = 1.2U_{eq}(C). Soft similarity restraints were applied to anisotropic thermal values of the atoms of one triazole rings (N10 N11 N12 C17 C18).

Refinement of (2).

The ADDSYMM analysis, as it implemented in PLATON, was suggestive of the orthorhombic-I lattice. Solution in the appropriate space groups (*i.e.*, *Immm*) was possible, however, the subsequent refinement afforded a poorly converged models (R1 > 0.12) involving disorder of the organic ligands and comprising many NPD carbon and nitrogen atoms. The stable and well-refinable model was found for orthorhombic-P space group *Pnnm*.

Most problems with the structure refinement were associated with the disorder of molybdate anions. In the environment of (μ_4-O)Cu_4 cluster, three $(MoO_4)^{2-}$ anions are disordered over four positions (Figure S1), in such a way that the anions referenced by Mo2 and Mo3 atoms are ordered and two anions (Mo1 and Mo4) are equally disordered by symmetry over two positions (overlapping with the disordered solvate water molecules). All atoms corresponding to these $(MoO_4)^{2-}$ anions were refined anisotropically. Additionally, the residual electron density features relatively significant peak (about 4 e $Å^3$) near Mo2 atom. Therefore, this molybdate ion (Mo2) was also regarded as disordered, with contributions from the major component (Mo2) and two symmetry-related minor components (Mo2A). Refinement of partial occupancies led to 0.846(6) for Mo2 and 2 × 0.077(3) for Mo2A. It was not possible to resolve the disorder for corresponding oxygen atoms, and therefore

this molybdate anion was left as is, with the above partial occupancy for Mo2 and with "ghost" Mo2A atom (refined anisotropically).

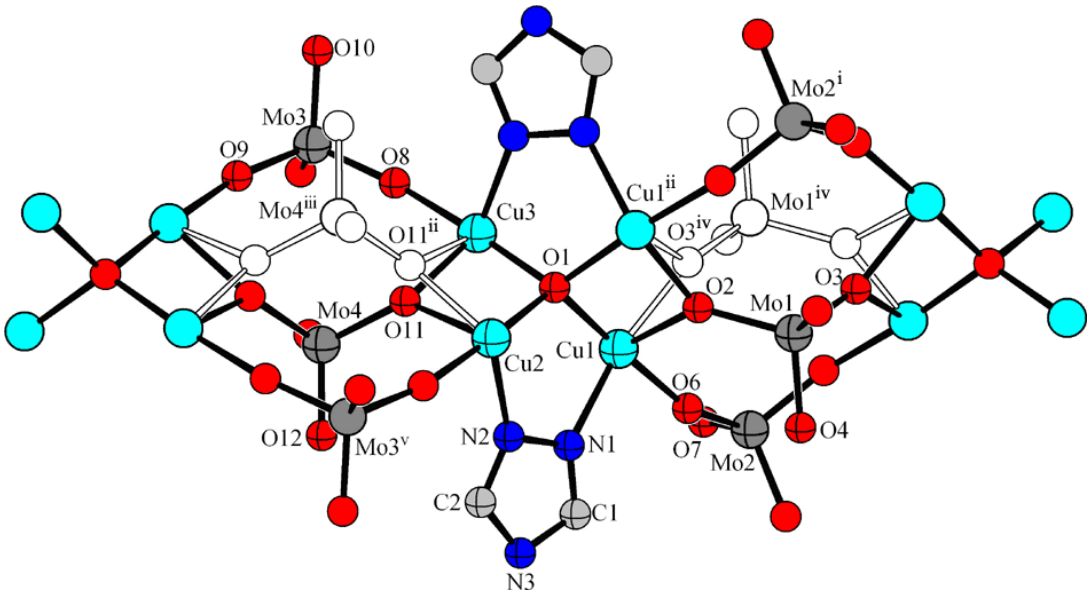

Figure S1. Fragment of the structure of (**2**) showing the mode of interconnection of the (μ_4-O)Cu_4 clusters by molybdate anions. Each inorganic link between the clusters comprises three MoO_4^{2-} anions, one of which is equally disoredered over two symmetry-related positions (i.e. Mo1 and $Mo1^{iv}$; Mo4 and $Mo4^{iii}$). Symmetry codes: (i) -x, -y+1, -z; (ii) x, y, -z; (iii) -x+1, -y+1, -z; (iv) -x, -y+1, z; (v) -x+1, -y+1, z.

In the region of solvate water molecules, two molecules (O1W and O2W) are ordered, these oxygen atoms were refined anisotropically. Oxygen atoms of other water molecules were left isotropic, in view of high thermal parameters and disorder. Atoms O4W-O7W were refined with partial occupancy factors of 0.5. Some of them are components of the disorder by two closely separated positions (e.g. O6W...O7W = 1.12 Å). Considering disorder in the solvent region, as well disorder of $(MoO_4)^{2-}$ anions (as hydrogen-bond acceptors), attribution of water hydrogen atoms was impossible. These hydrogen atoms were not added to the refinement.

Refinement of (3) and (4).

Refinement of the structure was essentially standard. For (**3**), the CH-hydrogen atoms were added geometrically and refined as riding, with U_{iso} = 1.2U_{eq}(C). The hydrogen atoms of solvate water molecule were located and included with fixed *d* (O-H) = 0.85 Å and U_{iso} = 1.5U_{eq} (O). For (**4**), the OH-hydrogen atoms was located (O-H = 0.79 Å) and then fixed with U_{iso} = 1.5U_{eq} (O).

Table S1. Crystal data for compounds **1-4**.

	1	**2**	**3**	**4**
Formula	$C_{56}H_{72}Cu_2Mo_8N_{24}O_{26}$	$C_{28}H_{51}Cu_4Mo_3N_{12}O_{20.50}$	$C_{28}H_{38}Cu_2Mo_2N_{12}O_8$	$Cu_3H_2Mo_2O_{10}$
T / K	213(2)	296(2)	213(2)	296(2)
M	2391.98	1425.79	989.66	544.52
Crystal system	Triclinic	Orthorhombic	Orthorhombic	Triclinic
Space group, Z	$P\bar{1}$, 1	*Pnnm*, 4	$P2_12_12_1$, 4	$P\bar{1}$, 1
a / Å	12.1133(4)	16.3312(12)	9.3560(7)	5.3507(2)
b / Å	12.7626(5)	22.4553(14)	11.5131(7)	5.5765(3)
c / Å	12.9724(5)	12.4140(7)	31.1479(17)	7.6182(4)
α / °	83.839(3)	90	90	103.810(3)
β / °	67.379(3)	90	90	106.336(3)
γ / °	81.747(3)	90	90	97.228(3)
V / Å^3	1829.06(12)	4552.5(5)	3355.1(4)	207.240(17)
μ(Mo-Kα) / mm^{-1}	1.988	2.722	2.051	10.551
D_c / g cm^{-3}	2.172	2.080	1.959	4.363
θ_{max} (°)	25.68	25.35	27.87	28.55
Meas / Unique reflns	17617 / 6907	15936 / 4280	23137 / 7931	2281 / 1034
Parameters refined	523	361	469	71
R1, wR2 [I > 2σ(I)]	0.060, 0.103	0.065, 0.126	0.028, 0.046	0.030, 0.057
R_1, wR_2 (all data)	0.122, 0.119	0.154, 0.155	0.045, 0.048	0.036, 0.060
Goof on F^2	0.903	1.048	0.800	1.116
Max, min / peak e Å^{-3}	0.93, -1.23	0.99, -1.16	1.00, -0.86	0.917, -0.825

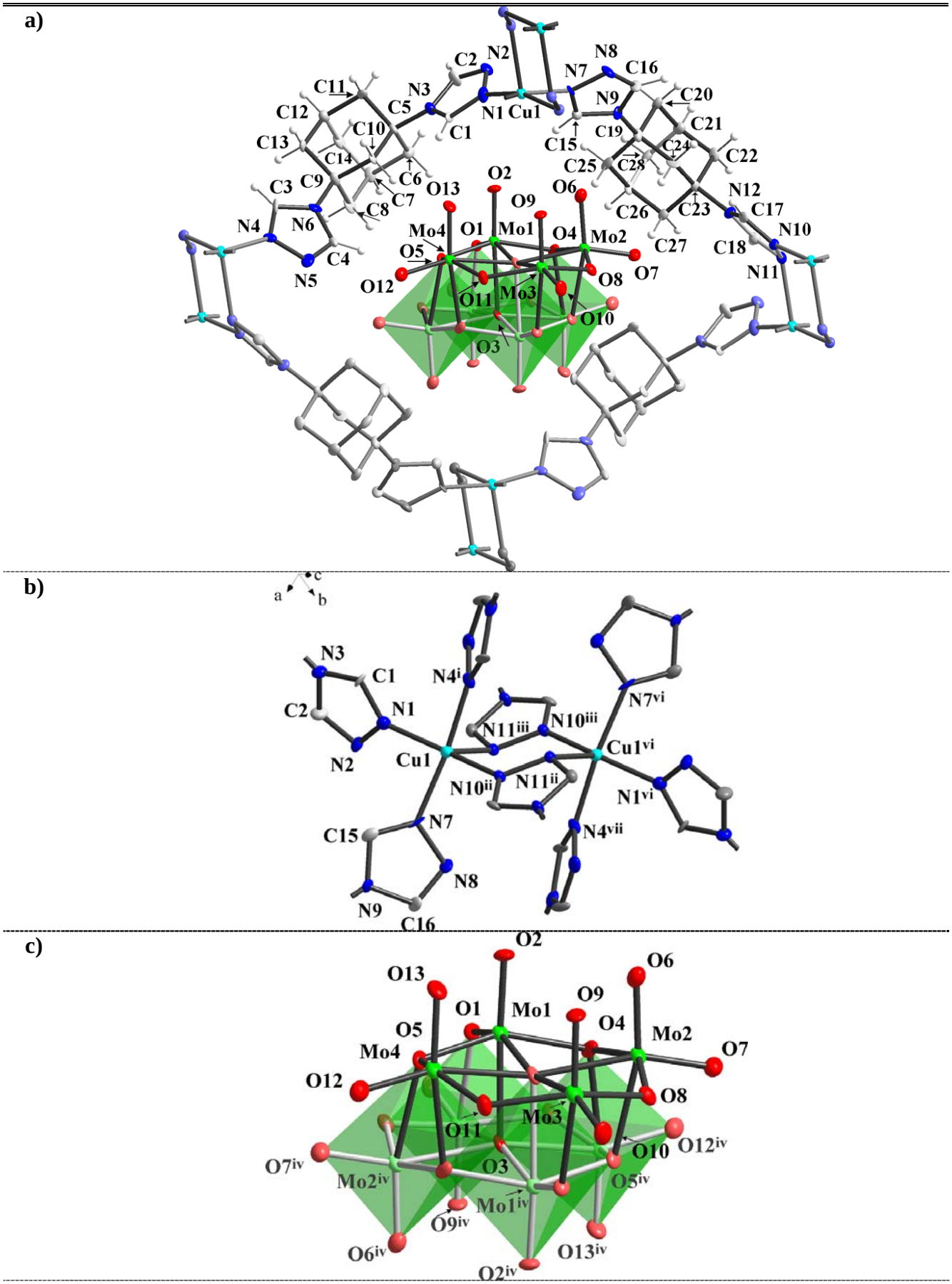

Figure S2. **a)**, **b)**, **c)** Crystal structure and labeling scheme for $[Cu_2(tr_2ad)_4](Mo_8O_{26})$, (**1**). Ellipsoids are shown at the 50% probability level. Symmetry codes: (i) -x, -y+1, -z+2; (ii) -x+1, -y+2, -z+2; (iii) x-1, y, z; (iv) -x+1, -y+1, -z+2; (v) x+1, y, z; (vi) -x, 2-y, 2-z; (vii) x, 1+y, z.

Table S2. Selected bond lengths (Å) and angles (°) for **1**.

$[Cu_2(tr_2ad)_4](Mo_8O_{26})$, (**1**), symmetry codes: (i) -x, -y+1, -z+2; (ii) -x+1, -y+2, -z+2; (iii) x-1, y, z; (iv) -x+1, -y+1, -z+2; (v) x+1, y, z.

Cu(1)-N(4)i	1.968(6)	Cu(1)-N(10)ii	2.002(7)
Cu(1)-N(1)	1.976(7)	Cu(1)-N(11)iii	2.247(7)
Cu(1)-N(7)	1.992(6)		
N(4)i-Cu(1)-N(1)	88.2(3)	N(7)-Cu(1)-N(10)ii	90.3(3)
N(4)i-Cu(1)-N(7)	169.5(3)	N(4)i-Cu(1)-N(11)iii	89.1(2)
N(1)-Cu(1)-N(7)	90.0(3)	N(1)-Cu(1)-N(11)iii	95.1(3)
N(4)i-Cu(1)-N(10)ii	88.4(3)	N(7)-Cu(1)-N(11)iii	101.4(2)
N(1)-Cu(1)-N(10)ii	163.5(3)	N(10)ii-Cu(1)-N(11)iii	101.1(3)
Mo(1)-O(2)	1.693(5)	Mo(3)-O(9)	1.700(5)
Mo(1)-O(1)	1.747(5)	Mo(3)-O(10)	1.708(5)
Mo(1)-O(4)	1.944(5)	Mo(3)-O(11)	1.896(5)
Mo(1)-O(5)	1.954(5)	Mo(3)-O(8)	1.925(5)
Mo(1)-O(3)iv	2.150(6)	Mo(3)-O(1)iv	2.277(5)
Mo(1)-O(3)	2.355(5)	Mo(4)-O(12)	1.694(5)
Mo(2)-O(7)	1.701(5)	Mo(4)-O(13)	1.697(5)
Mo(2)-O(6)	1.707(6)	Mo(4)-O(11)	1.919(6)
Mo(2)-O(8)	1.904(5)	Mo(4)-O(5)	2.006(5)
Mo(2)-O(4)	2.002(6)	Mo(4)-O(3)iv	2.307(5)
Mo(2)-O(3)iv	2.285(5)	Mo(4)-O(4)iv	2.339(5)
Mo(2)-O(5)iv	2.352(5)		

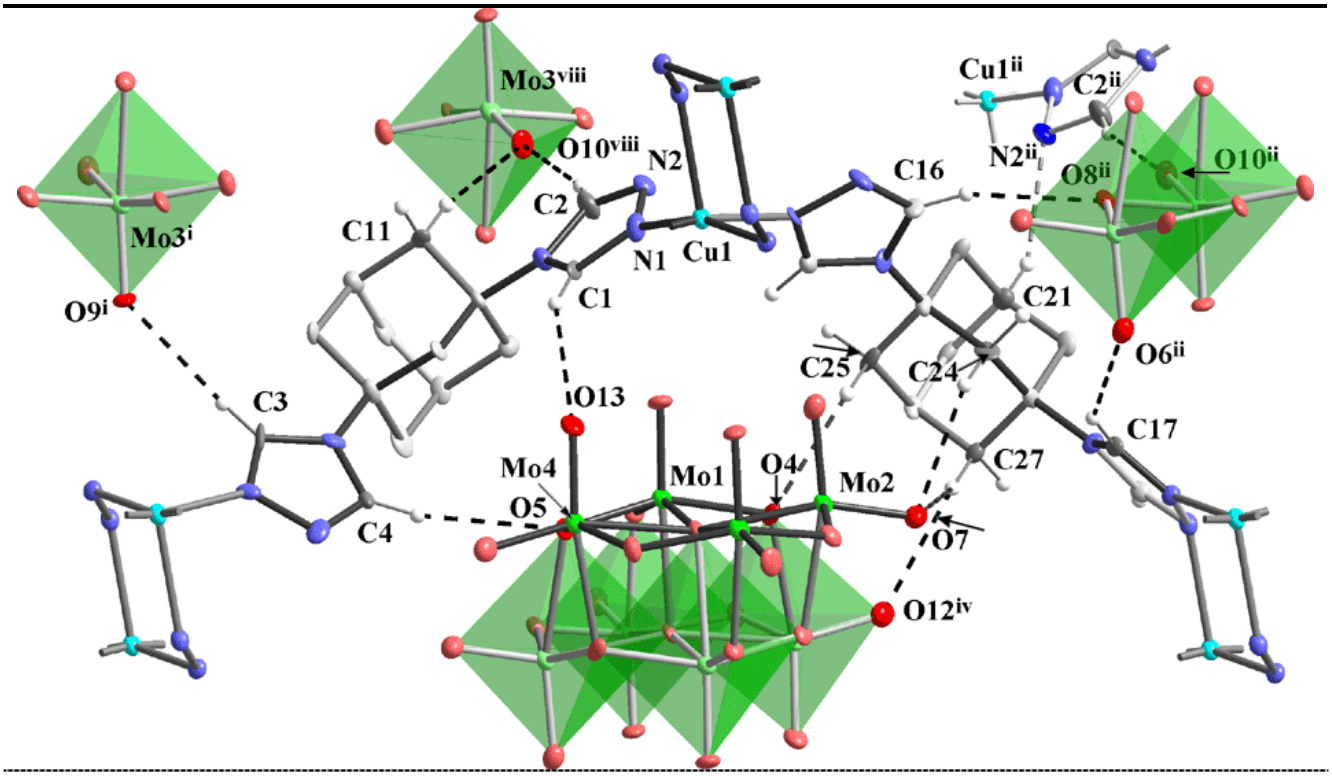

Figure S3. Illustration of the C-H…O and C-H…N(*tr*) interactions in the crystal structure of $[Cu_2(tr_2ad)_4](Mo_8O_{26})$, (**1**). Symmetry codes: (i) (i) -x, -y+1, -z+2; (ii) -x+1, -y+2, -z+2; (iii) x-1, y, z; (iv) -x+1, -y+1, -z+2; (v) x+1, y, z; (vi) -x, 2-y, 2-z; (vii) x, 1+y, z; (viii) x, y, -1+z.

Table S3. Hydrogen bonding scheme in the crystal structure of **1** (Å, °).[S4, S5]

D-H···*A*	H···*A*	*D*···*A*	*D*-H···*A*
C(1)--H(1) ..O(13)	2.58	3.4227	149
C(2)--H(2) ..O(10)viii	2.34	3.2552	163
C(3)--H(3) ..O(9)i	2.51	3.3766	153
C(4)--H(4) ..O(5)	2.58	3.5058	168
C(11)--H(11A)..O(10)viii	2.37	3.3378	169
C(16) --H(16) ..O(8)ii	2.52	3.4109	158
C(17) --H(17) ..O(6)ii	2.45	3.2535	144
C(21) --H(21) ..N(2)ii	2.50	3.3979	151
C(24) --H(24B) ..O(7)	2.53	3.4048	149
C(25) --H(25B) ..O(4)	2.58	3.4892	154
C(27) --H(27B) ..O(7)	2.54	3.4134	149
C(27) --H(27B) ..O(12)iv	2.52	3.3100	138

(i) -x, -y+1, -z+2; (ii) -x+1, -y+2, -z+2; (iii) x-1, y, z; (iv) -x+1, -y+1, -z+2; (v) x+1, y, z; (vi) -x, 2-y, 2-z; (vii) x, 1+y, z; (viii) x, y, -1+z.

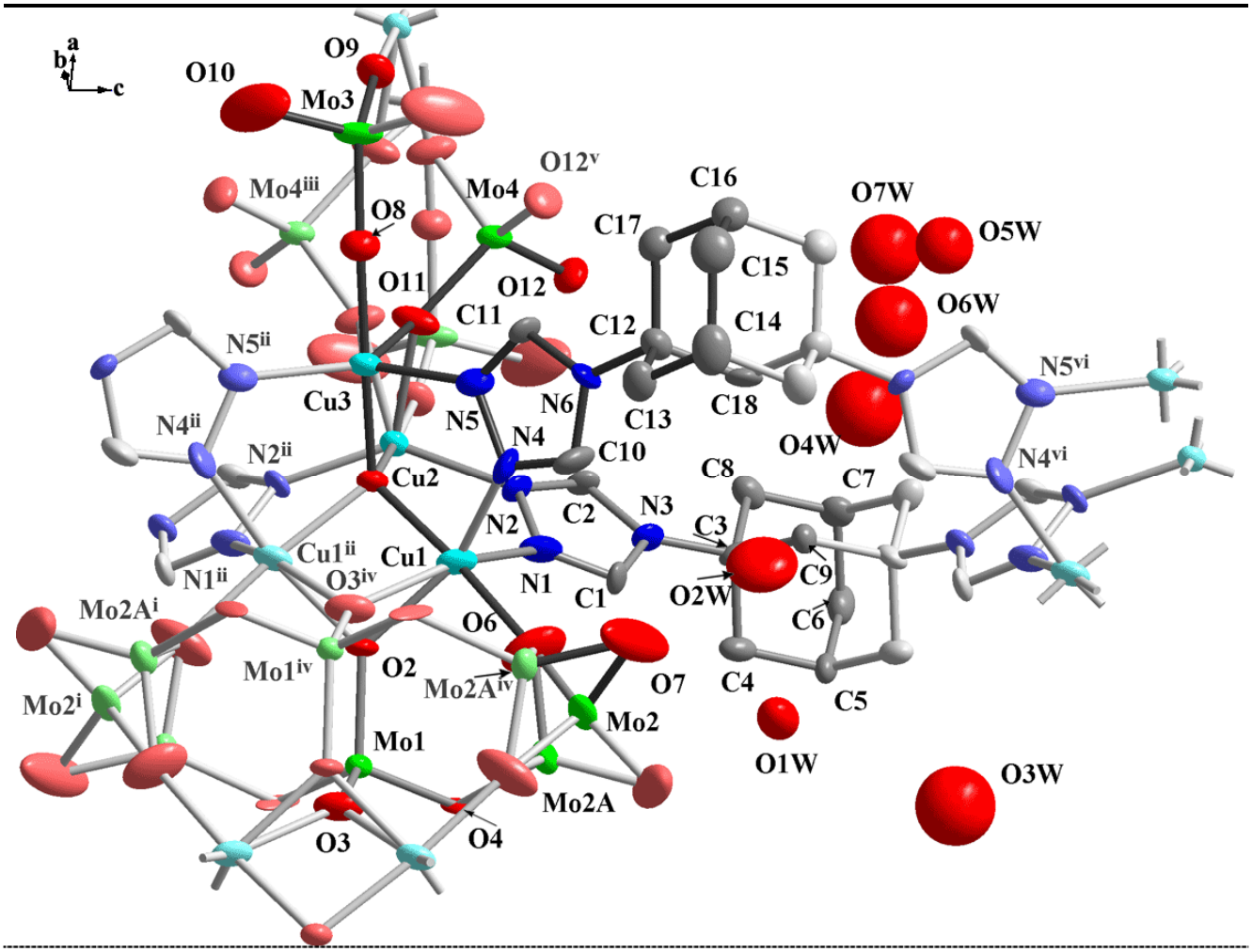

Figure S4. Crystal structure and labeling scheme for $[Cu_4(\mu_4\text{-}O)(tr_2ad)_2(MoO_4)_3]\cdot 7.5H_2O$, (**2**); symmetry codes: (i) -x, -y+1, -z; (ii) x, y, -z; (iii) -x+1, -y+1, -z; (iv) -x, -y+1, z; (v) -x+1, -y+1, z; (vi) x, y, -z+1.

Table S4. Selected bond lengths (Å) and angles (°) for **2**.

$[Cu_4(\mu_4\text{-}O)(tr_2ad)_2(MoO_4)_3]\cdot 7.5H_2O$, (**2**), (symmetry codes: (i) -x, -y+1, -z; (ii) x, y, -z; (iii) -x+1, -y+1, -z; (iv) -x, -y+1, z; (v) -x+1, -y+1, z; (vi) x, y, -z+1).

Cu(1)-O(6)	1.924(9)	Cu(2)-O(1)	1.960(9)
Cu(1)-O(1)	1.955(6)	Cu(2)-N(2)	2 x 2.005(8)
Cu(1)-O(2)	1.964(12)	Cu(2)-O(11)	2 x 2.091(11)
Cu(1)-O(3)i	2.028(14)	Cu(3)-O(8)	1.938(10)
Cu(1)-N(4)	2.078(10)	Cu(3)-O(1)	1.966(9)
Cu(1)-N(1)	2.093(9)	Cu(3)-N(5)	2 x 2.009(9)
Cu(2)-O(9)iii	1.938(10)	Cu(3)-O(11)	2 x 2.067(11)
Mo(1)-O(4)	2 x 1.726(13)	Mo(4)-O(11)	2 x 1.798(8)
Mo(2)-O(7)	2 x 1.732(14)	Mo(1)-O(3)	1.80(2)
Mo(2)-O(6)	2 x 1.718(8)	Mo(1)-O(2)	1.819(17)

Table S4. continued

Mo(3)-O(10)	2 x 1.733(11)	Mo(3)-O(8)	1.746(10)
Mo(4)-O(12)	2 x 1.712(13)	Mo(3)-O(9)	1.733(10)
O(6)-Cu(1)-O(1)	175.2(4)	O(9)iii-Cu(2)-O(1)	176.6(4)
O(6)-Cu(1)-O(2)	90.9(5)	N(2)ii-Cu(2)-N(2)	137.2(5)
O(1)-Cu(1)-O(2)	84.5(4)	O(1)-Cu(2)-N(2)	2 x 92.9(3)
O(6)-Cu(1)-O(3)i	94.2(5)	O(9)iii-Cu(2)-N(2)	2 x 88.4(3)
O(1)-Cu(1)-O(3)i	83.1(5)	O(9)iii-Cu(2)-O(11)	2 x 91.8(4)
O(2)-Cu(1)-O(3)i	37.1(7)	O(1)-Cu(2)-O(11)	2 x 84.8(4)
O(6)-Cu(1)-N(4)	92.7(4)	N(2)ii-Cu(2)-O(11)	2 x 123.3(4)
O(1)-Cu(1)-N(4)	91.9(3)	N(2)-Cu(2)-O(11)	2 x 99.4(4)
O(2)-Cu(1)-N(4)	142.0(6)	O(8)-Cu(3)-O(1)	175.5(4)
O(3)i-Cu(1)-N(4)	104.8(6)	O(8)-Cu(3)-N(5)	2 x 89.1(3)
O(6)-Cu(1)-N(1)	88.5(4)	O(1)-Cu(3)-N(5)	2 x 92.7(3)
O(1)-Cu(1)-N(1)	92.1(3)	O(8)-Cu(3)-O(11)	2 x 90.3(4)
O(2)-Cu(1)-N(1)	117.1(6)	O(1)-Cu(3)-O(11)	2 x 85.3(4)
O(3)i-Cu(1)-N(1)	154.0(6)	N(5)-Cu(3)-O(11)	2 x 101.1(4)
N(4)-Cu(1)-N(1)	100.9(3)	N(5)ii-Cu(3)-O(11)	2 x 125.3(4)
O(4)ii-Mo(1)-O(4)	108.0(10)	Cu(2)-O(1)-Cu(3)	97.2(4)
O(4)-Mo(1)-O(3)	2 x 109.6(6)	O(3)i-O(2)-Mo(1)	114.9(15)
O(4)-Mo(1)-O(2)	2 x 108.3(5)	O(3)i-O(2)-Cu(1)	2 x 74.1(9)
O(3)-Mo(1)-O(2)	113.0(8)	Mo(1)-O(2)-Cu(1)	2 x 133.2(4)
O(6)iv-Mo(2)-O(6)	111.6(7)	Cu(1)-O(2)-Cu(1)ii	93.6(7)
O(6)iv-Mo(2)-O(7)	2 x 109.5(7)	O(2)i-O(3)-Mo(1)	132.1(16)
O(6)-Mo(2)-O(7)	2 x 106.4(5)	O(2)i-O(3)-Cu(1)iv	2 x 68.7(9)
O(7)-Mo(2)-O(7)iv	113.6(11)	Mo(1)-O(3)-Cu(1)iv	2 x 134.0(5)
O(9)-Mo(3)-O(10)	2 x 107.4(4)	Cu(1)iv-O(3)-Cu(1)i	89.8(8)
O(10)-Mo(3)-O(10)ii	114.4(9)	Mo(2)-O(6)-Cu(1)	156.7(6)
O(9)-Mo(3)-O(8)	112.2(5)	Mo(3)-O(8)-Cu(3)	171.4(6)
O(10)-Mo(3)-O(8)	2 x 107.8(4)	Mo(3)-O(9)-Cu(2)iii	167.1(7)

Table S4. continued			
O(12)-Mo(4)-O(12)v	110.7(10)	O(11)ii-O(11)-Mo(4)	127.9(4)
O(12)-Mo(4)-O(11)	2 x 110.2(6)	O(11)ii-O(11)-Cu(3)	77.9(3)
O(12)v-Mo(4)-O(11)	2 x 110.6(7)	Mo(4)-O(11)-Cu(3)	131.1(7)
O(11)-Mo(4)-O(11)v	104.3 (8)	Mo(4)-O(11)-Cu(2)	131.5(7)
Cu(1)ii-O(1)-Cu(1)	94.1(4)	Cu(3)-O(11)-Cu(2)	90.2(3)
Cu(1)-O(1)-Cu(2)	2 x 116.8(3)	Cu(3)-O(11)-Mo(4)iii	102.8(5)
Cu(1)-O(1)-Cu(3)	2 x 116.8(3)	Cu(2)-O(11)-Mo(4)iii	103.3(5)

Cu(2)...Cu(3) 2.946(2) Å, Cu(1)...Cu(1)ii 2.864(3) Å

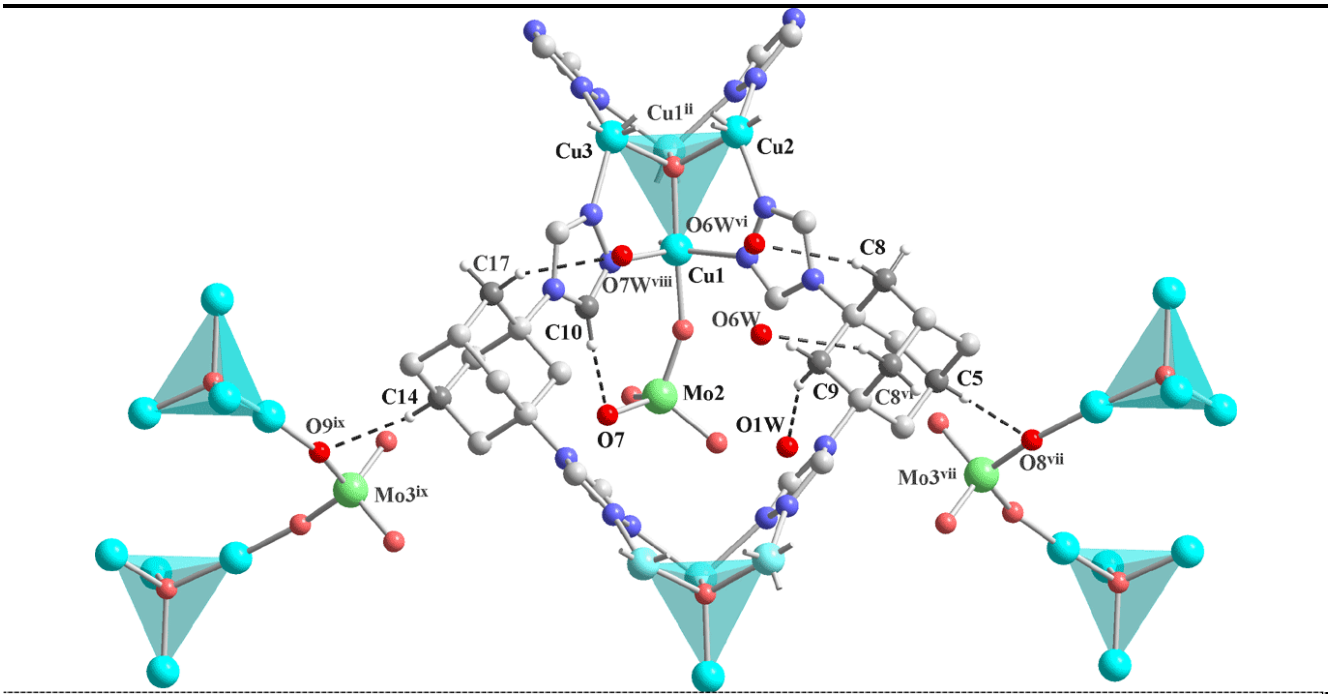

Figure S5. Illustration of the C-H…O hydrogen bond contacts in the crystal structure **2**; symmetry codes: (vi) x, y, -z+1; (vii) 0.5-x, -0.5+y, 0.5-z; (viii) -x+1, -y+1, -z+1; (ix) -0.5+x, 1.5-y, 0.5-z.

Table S5. Selected hydrogen bond interactions in the crystal structure of **2** (Å, °).[S4, S5]

D-H···*A*	H···*A*	*D*···*A*	*D*-H···*A*
C(5)--H(5) ..O(8)vii	2.42	3.4003	179
C(8)--H(8B) ..O(6W)vi	2.56	3.4471	151
C(9)--H(9B) ..O(1W)	2.49	3.4088	157
C(10)--H(10) ..O(7)	2.18	3.0550	157
C(14)--H(14) ..O(9)ix	2.47	3.4265	166
C(17)--H(17B) ..O(7W)viii	2.51	3.3981	152

(vi) x, y, -z+1; (vii) 0.5-x, -0.5+y, 0.5-z; (viii) -x+1, -y+1, -z+1; (ix) -0.5+x, 1.5-y, 0.5-z.

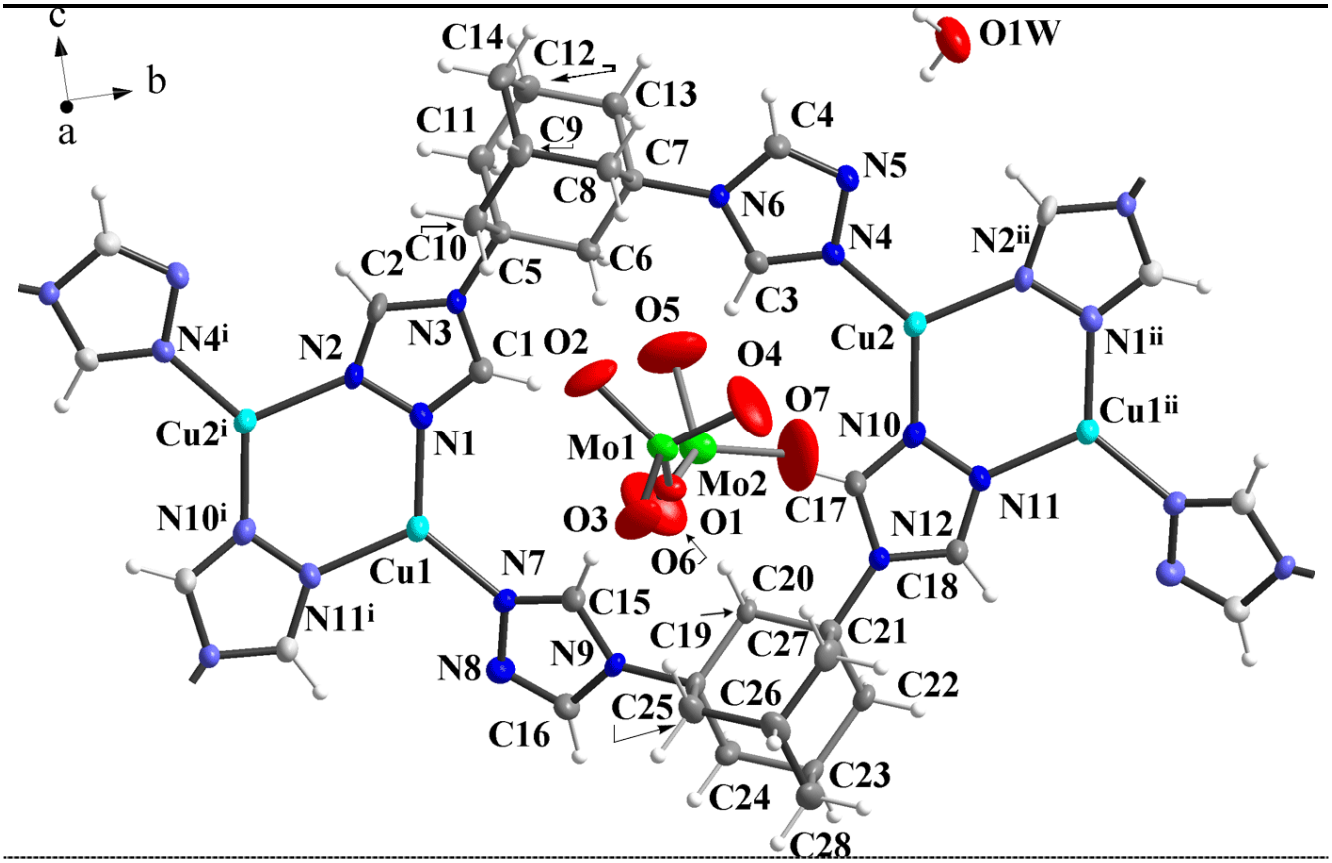

Figure S6. Crystal structure and labeling scheme for $[Cu_2(tr_2ad)_2](Mo_2O_7)\cdot H_2O$, (**3**). Ellipsoids are shown at the 50% probability level (symmetry codes: (i) x, -1+y, z; (ii) x, 1+y, z).

Table S6. Selected bond lengths (Å) and angles (°) for **3**.

$[Cu_2(tr_2ad)_2](Mo_2O_7)\cdot H_2O$, (**3**), (symmetry codes: (i) x, -1+y, z; (ii) x, 1+y, z).

Cu(1)-N(7)	1.934(3)	Cu(2)-N(4)	1.927(3)
Cu(1)-N(1)	1.965(3)	Cu(2)-N(10)	1.938(3)
Cu(1)-N(11)i	2.001(3)	Cu(2)-N(2)ii	2.002(3)
Mo(1)-O(3)	1.703(3)	Mo(2)-O(5)	1.690(3)
Mo(1)-O(2)	1.706(3)	Mo(2)-O(6)	1.698(4)
Mo(1)-O(4)	1.706(3)	Mo(2)-O(7)	1.719(4)
Mo(1)-O(1)	1.885(2)	Mo(2)-O(1)	1.897(2)
N(7)-Cu(1)-N(1)	127.83(11)	N(7)-Cu(1)-N(11)i	116.73(12)
N(1)-Cu(1)-N(11)i	114.74(11)	N(4)-Cu(2)-N(10)	132.09(12)
N(4)-Cu(2)-N(2)ii	115.15(12)	N(10)-Cu(2)-N(2)ii	112.61(12)
C(1)-N(1)-Cu(1)	130.3(2)□	N(2)-N(1)-Cu(1)	121.1(2)
C(2)-N(2)-Cu(2)i	128.4(2)	N(1)-N(2)-Cu(2)i	124.8(2)
C(3)-N(4)-Cu(2)	128.2(3)	N(5)-N(4)-Cu(2)	123.5(2)

Table S6. continued			
C(15)-N(7)-Cu(1)	129.5(2)	N(8)-N(7)-Cu(1)	122.5(2)
C(17)-N(10)-Cu(2)	127.2(2)	N(11)-N(10)-Cu(2)	125.1(2)
C(18)-N(11)-Cu(1)ii	130.9(2)	N(10)-N(11)-Cu(1)ii	121.5(2)
O(3)-Mo(1)-O(2)	107.78(15)	O(3)-Mo(1)-O(4)	108.9(2)
O(2)-Mo(1)-O(4)	108.7(2)	O(3)-Mo(1)-O(1)	111.60(13)
O(2)-Mo(1)-O(1)	109.26(15)	O(4)-Mo(1)-O(1)	110.45(14)
O(5)-Mo(2)-O(6)	112.9(2)	O(5)-Mo(2)-O(7)	108.2(2)
O(6)-Mo(2)-O(7)	107.6(2)	O(5)-Mo(2)-O(1)	109.46(16)
O(6)-Mo(2)-O(1)	108.64(16)	O(7)-Mo(2)-O(1)	110.06(16)
Mo(1)-O(1)-Mo(2)	136.46(13)		

Table S7. Hydrogen bonding scheme in the crystal structure of **3** (Å, °).[S4, S5]

D-H···*A*	H···*A*	*D*···*A*	*D*-H···*A*
O(1W)-H(1W) ..N(5)	2.24	2.9675	144
O(1W)-H(2W) ..O(2)iii	2.02	2.8361	160
C(1)-H(1) ..O(3)iv	2.51	3.4115	162
C(2)ii-H(2)ii ..O(1W)	2.52	3.4287	163
C(4)-H(4) ..O(2)iii	2.39	3.2367	149
C(6)-H(6A) ..O(2)	2.42	3.3685	163
C(6)-H(6B) ..O(5)iv	2.43	3.2822	145
C(8)-H(8B) ..O(5)	2.50	3.3384	143
C(15)-H(15) ..O(6)	2.47	3.3390	154
C(16)-H(16) ..O(4)(v)	2.52	3.2638	136
C(18)-H(18) ..O(1)(vi)	2.37	3.2815	164
C(22)-H(22A) ..O(1)(vi)	2.45	3.3972	162

(i) x, -1+y, z; (ii) x, 1+y, z; (iii) -0.5+x, 0.5-y, 1-z; (iv) -1+x, y, z; (v) 1-x, -0.5+y, 0.5-z; (vi) 1-x, 0.5+y, 0.5-z.

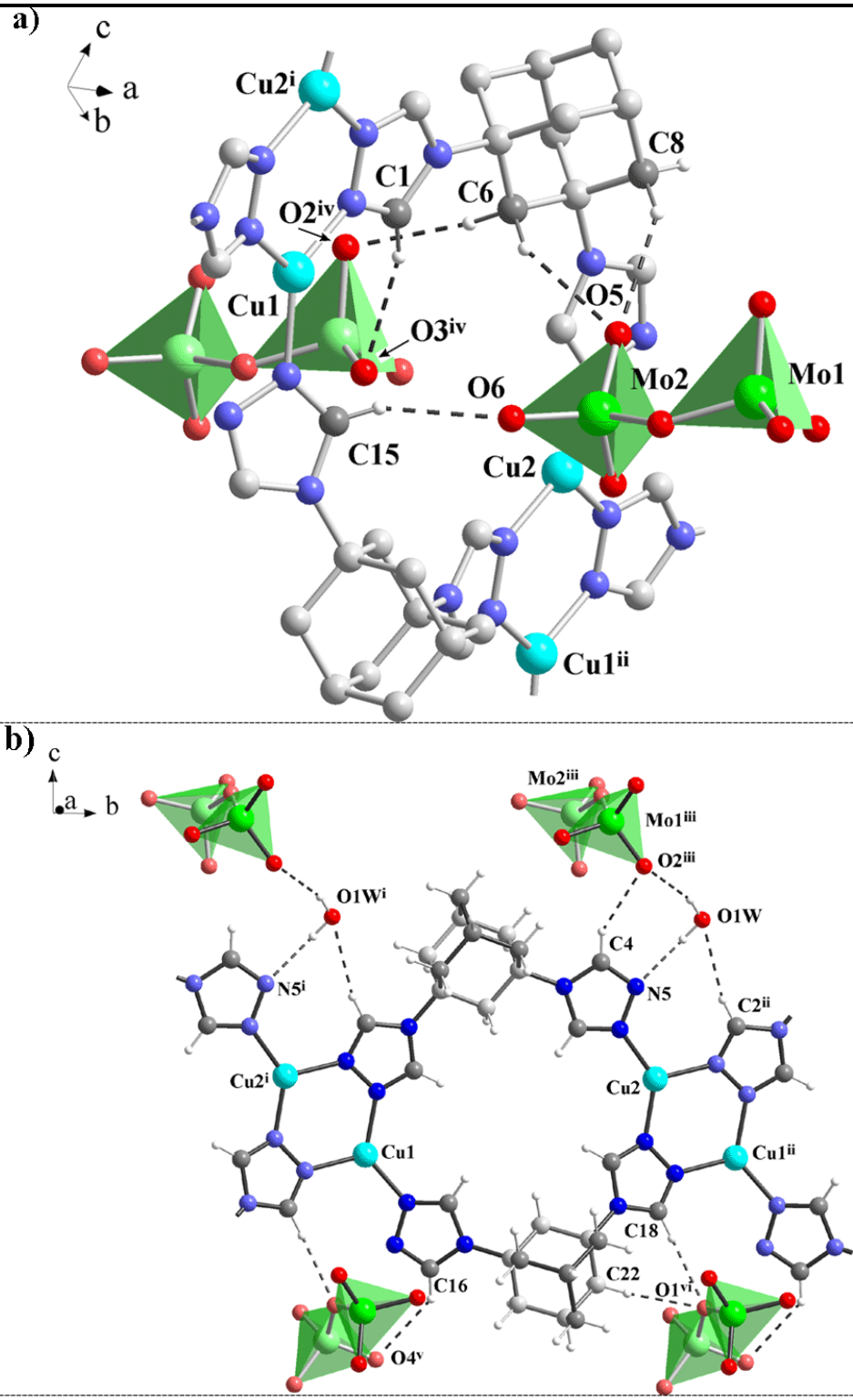

Figure S7. H-bonding interactions between organic ligands, water molecules and dimolybdate anions in the crystal structure of $[Cu_2(tr_2ad)_2](Mo_2O_7)\cdot H_2O$, (**3**); symmetry codes: (i) x, -1+y, z; (ii) x, 1+y, z; (iii) -0.5+x, 0.5-y, 1-z; (iv) -1+x, y, z; (v) 1-x, -0.5+y, 0.5-z; (vi) 1-x, 0.5+y, 0.5-z.

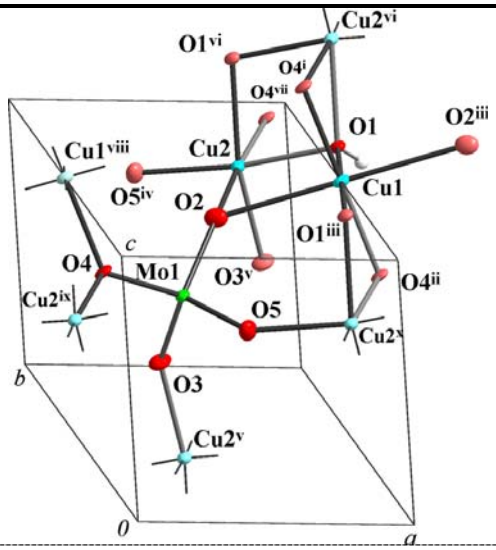

Figure S8. Crystal structure and labeling scheme for $[Cu_3(MoO_4)_2(OH)_2]$, (**4**). Ellipsoids are shown at the 50% probability level. Symmetry codes: (i) -x+1, -y+1, -z+2; (ii) x+1, y, z; (iii) -x+2, -y+1, -z+2; (iv) x, y+1, z; (v) -x+1, -y+1, -z+1; (vi) -x+2, -y+2, -z+2; (vii) x+1, y+1, z; (viii) x-1, y, z; (ix) x-1, y-1, z; (x) x, y-1, z.

a)

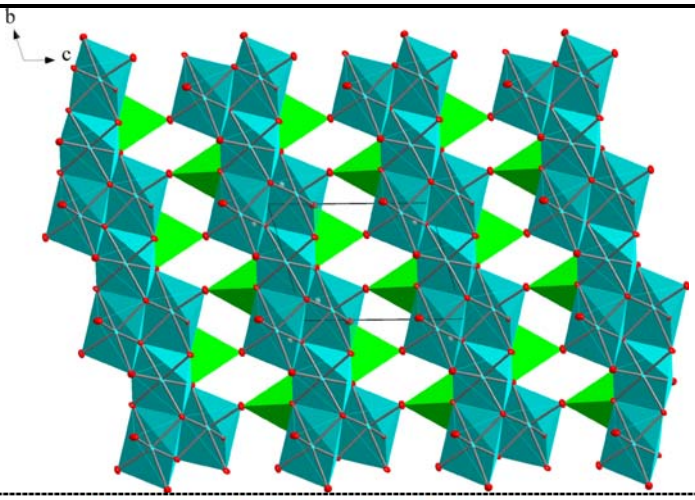

b)

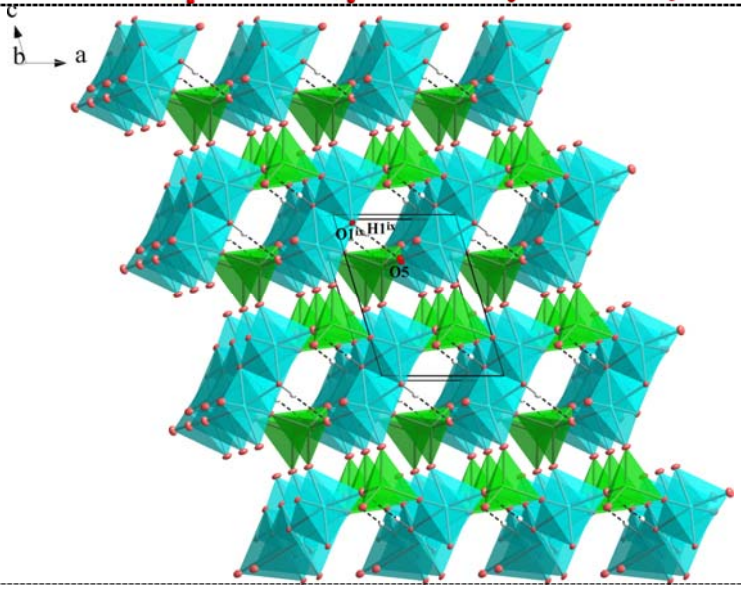

Figure S9. **a)** view of 3D network, $[Cu_3(MoO_4)_2(OH)_2]$ (**4**), in the *bc* plane; **b)** the O-H…O hydrogen-bonding interactions (O1(ix)-H1(ix)…O5 3.0516 Å, ∠O1(ix)-H1(ix)-O5 161.00°; symmetry code: (ix) *x*+1, *y*, *z*) in the crystal structure of **4**, viewed towards the (0 $\bar{3}$1) plane (CuO_6 octahedra shown in cyan, MoO_4 tetrahedra shown in green).

Table S8. Selected bond lengths (Å) and angles (°) for **4**.

$[Cu_3(MoO_4)_2(OH)_2]$, (**4**), symmetry codes: (i) -x+1, -y+1, -z+2; (ii) x+1, y, z; (iii) -x+2, -y+1, -z+2; (iv) x, y+1, z; (v) -x+1, -y+1, -z+1; (vi) -x+2, -y+2, -z+2; (vii) x+1, y+1, z; (viii) x-1, y, z; (ix) x-1, y-1, z; (x) x, y-1, z.

Cu(1)-O(4)	2 x 1.938(3)	O(1)vi-Cu(2)-O(2)	109.19(13)
Cu(1)-O(1)	2 x 1.985(3)	O(5)iv-Cu(2)-O(4)vii	94.17(14)
Cu(2)-O(5)iv	1.943(4)	O(3)v-Cu(2)-O(4)vii	88.24(13)
Cu(2)-O(3)v	1.950(3)	O(1)-Cu(2)-O(4)vii	92.87(13)
Cu(2)-O(1)	1.984(3)	O(1)vi-Cu(2)-O(4)vii	73.90(13)
Cu(2)-O(1)vi	2.000(3)	O(2)-Cu(2)-O(4)vii	176.47(11)
Cu(2)-O(2)	2.293(3)	O(2)-Mo(1)-O(3)	110.99(17)
Cu(2)-O(4)vii	2.418(3)	O(2)-Mo(1)-O(5)	109.65(17)
Mo(1)-O(2)	1.745(3)	O(3)-Mo(1)-O(5)	110.16(16)
Mo(1)-O(3)	1.753(3)	O(2)-Mo(1)-O(4)	108.29(15)
Mo(1)-O(5)	1.765(4)	O(3)-Mo(1)-O(4)	109.17(17)
Mo(1)-O(4)	1.785(3)	O(5)-Mo(1)-O(4)	108.51(16)
O(4)i-Cu(1)-O(4)ii	180	Cu(2)-O(1)-Cu(1)	107.63(15)
O(4)i-Cu(1)-O(1)	86.06(14)	Cu(2)-O(1)-Cu(2)vi	98.96(15)
O(1)-Cu(1)-O(1)iii	180	Cu(1)-O(1)-Cu(2)vi	104.06(15)
O(5)iv-Cu(2)-O(3)v	96.16(15)	Mo(1)-O(2)-Cu(2)	142.82(19)
O(5)iv-Cu(2)-O(1)	167.78(15)	Mo(1)-O(3)-Cu(2)v	144.1(2)
O(3)v-Cu(2)-O(1)	94.03(15)	Mo(1)-O(4)-Cu(1)viii	130.19(17)
O(5)iv-Cu(2)-O(1)vi	91.33(14)	Mo(1)-O(4)-Cu(2)ix	123.71(16)
O(3)v-Cu(2)-O(1)vi	161.11(15)	Cu(1)viii-O(4)-Cu(2)ix	91.65(13)
O(1)-Cu(2)-O(1)vi	81.04(15)	Mo(1)-O(5)-Cu(2)x	139.4(2)
O(5)iv-Cu(2)-O(2)	87.52(14)	Cu(1)-O(1)-H(1)	125.3
O(3)v-Cu(2)-O(2)	88.50(14)	Cu(2)vi-O(1)-H(1)	116.4
O(1)-Cu(2)-O(2)	86.03(13)	Cu(2)-O(1)-H(1)	101.0

* Cu(2)....Cu(2)vi 3.0291(11) Å

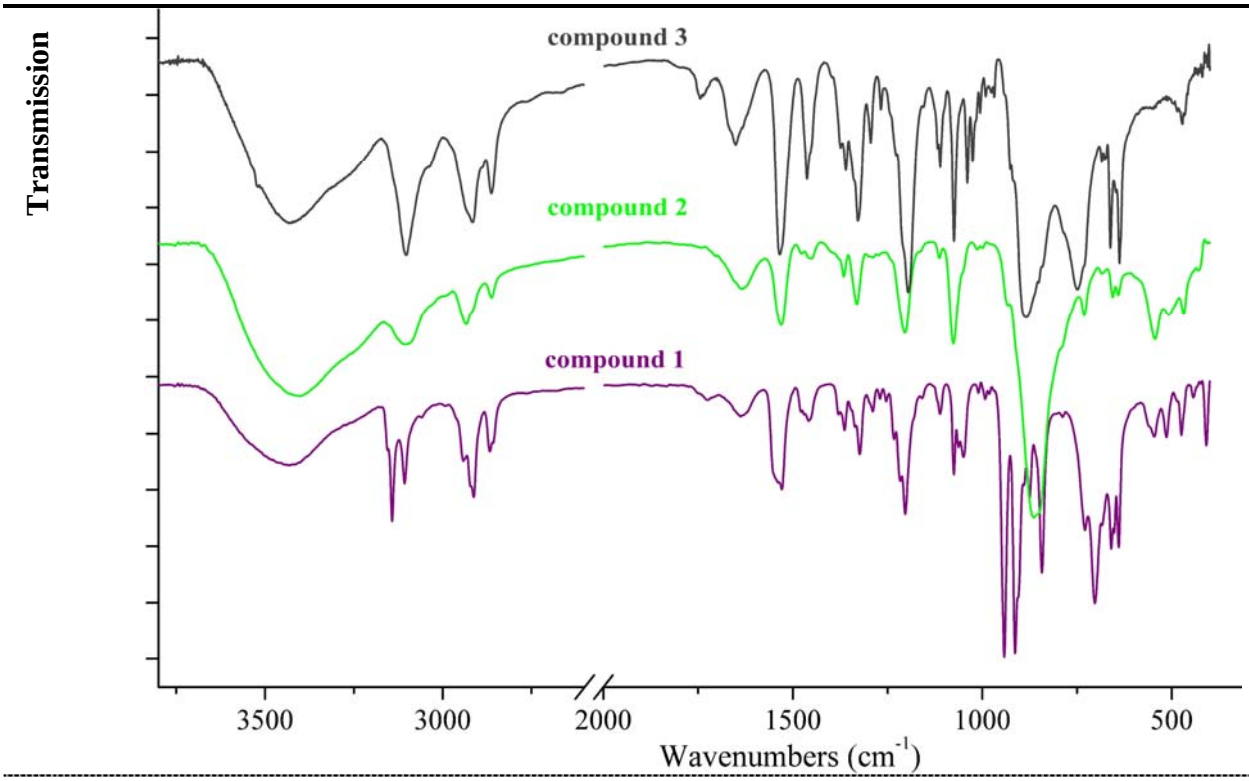

Figure S10. IR spectra of compounds **1-3**.

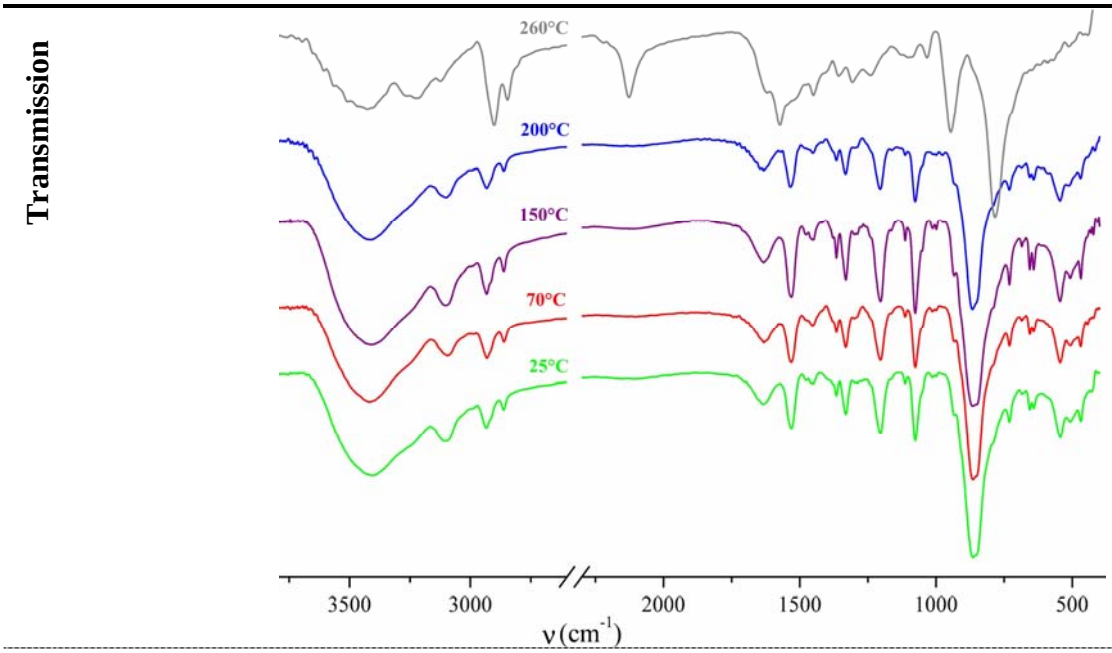

Figure S11. IR spectra of compound **2** recorded at rt and for a series of samples which were kept in air at elevated temperatures for 30 min.

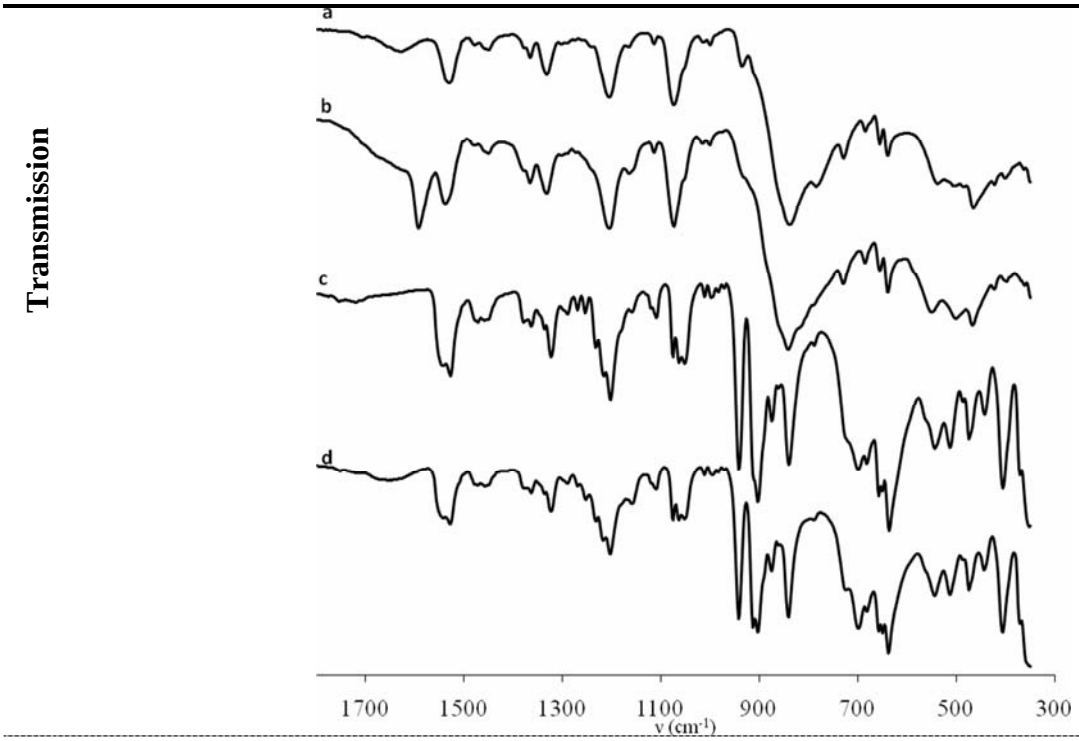

Figure S12. FT-IR ATR spectra for **2** (a), **2**-S (b), **1** (c) and **1**-S (d).

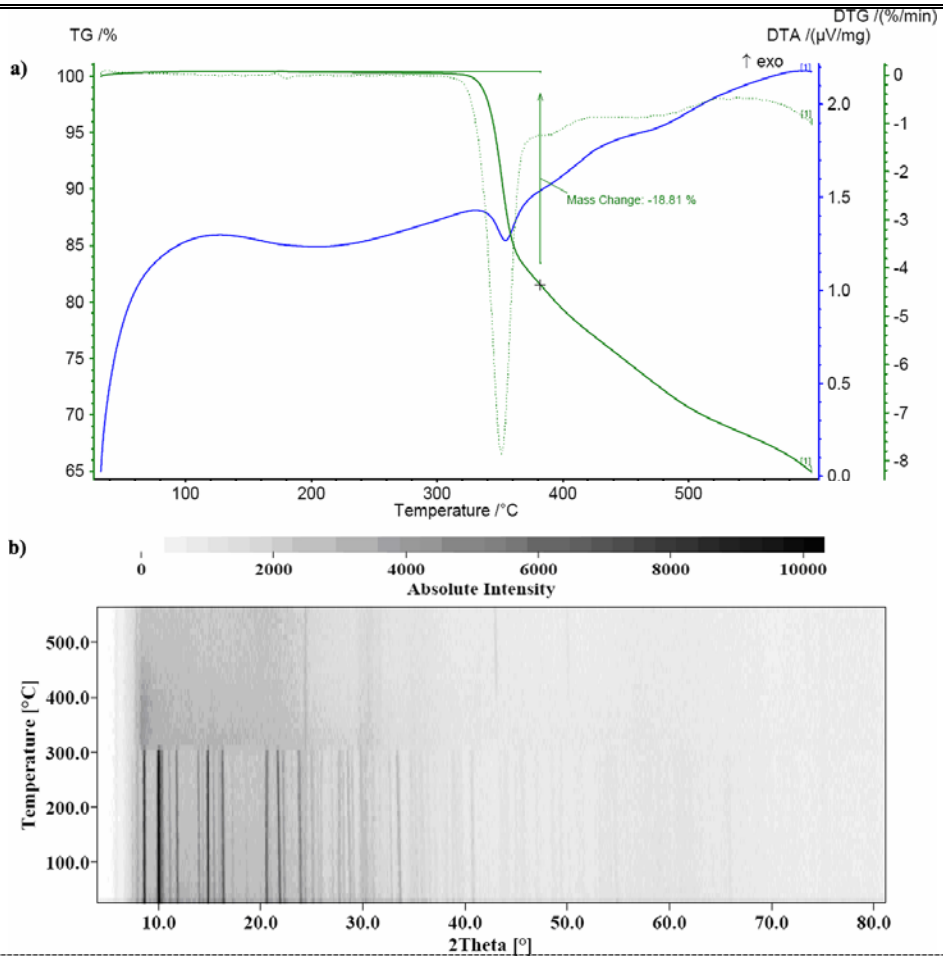

Figure S13. DTA/TG data and thermo-PXRD pattern (Cu-$K_{\alpha 1}$ radiation) for complex **1** showing a framework stability of up to 310 °C.

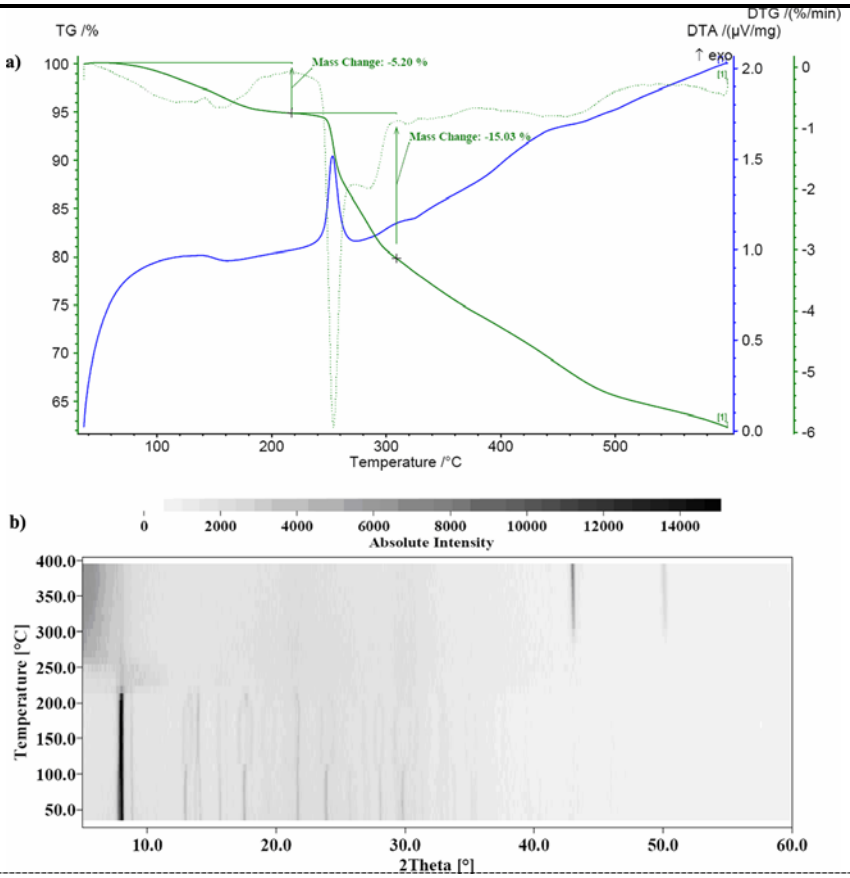

Figure S14. DTA/TG data and thermo-PXRD pattern (2θ = 5−60°) for compound **2** showing framework stability up to 210 °C.

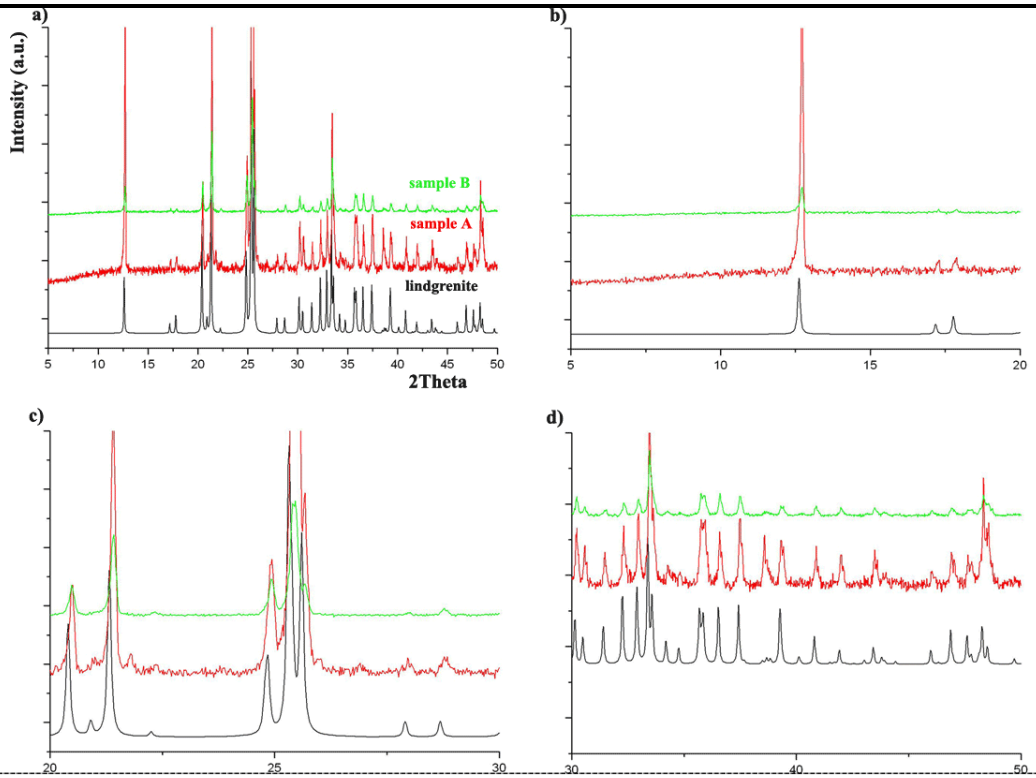

Figure S15. XRPD patterns of lindgrenite (simulated, black) and samples A, B (experimental: red, green, respectively) prepared from $Cu(OAc)_2{\cdot}H_2O/(NH_4)_6Mo_7O_{24}{\cdot}4H_2O$ at Cu^{II}: Mo^{VI} = 1:1 (red line: for 0.02 M Cu^{II}; green line for 0.06 M Cu^{II}). The data clearly confirm the formation of lindgrenite polymorph ($Cu_3(MoO_4)_2(OH)_2$, monoclinic space group).

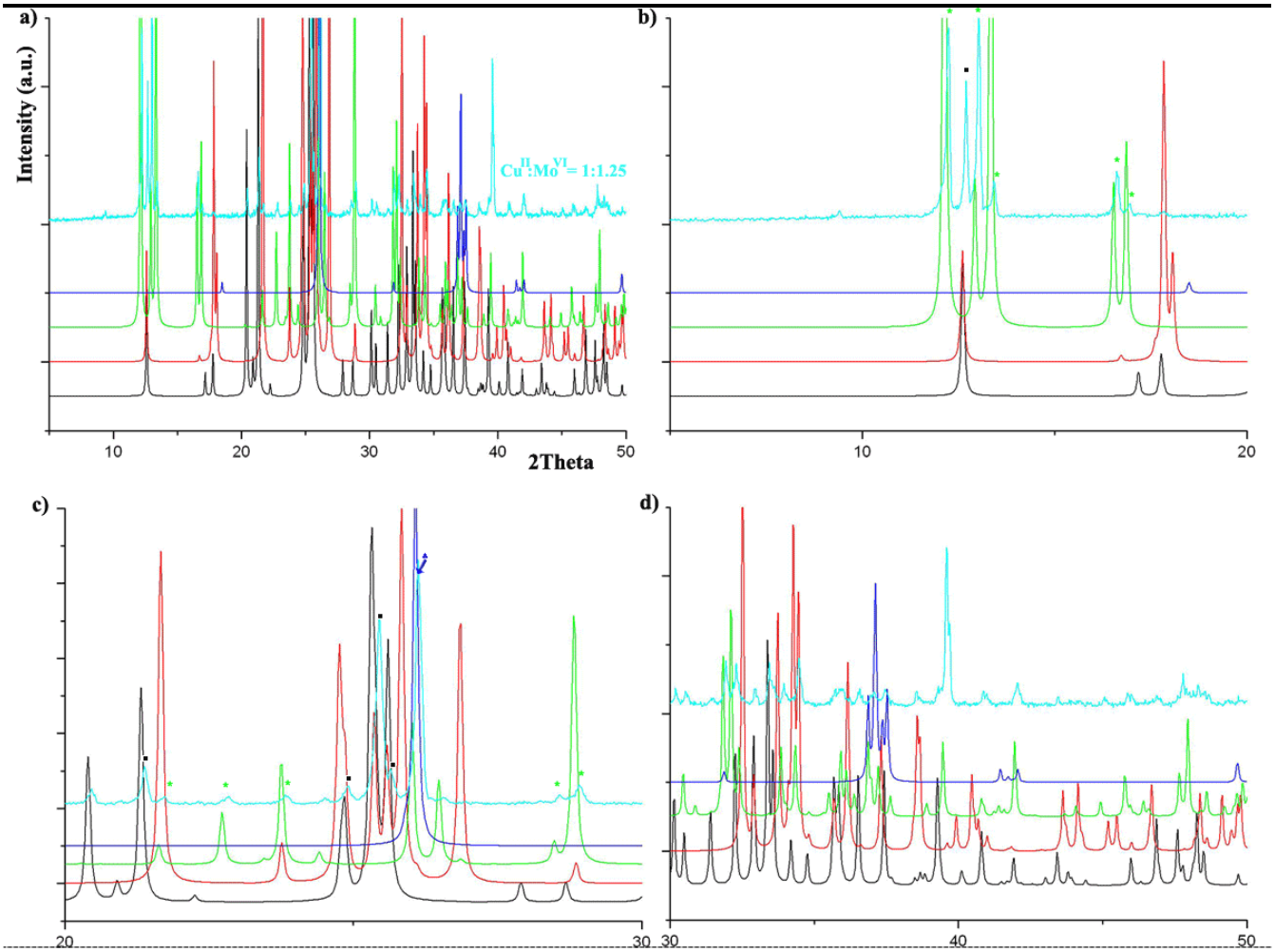

Figure S16. Simulated XRPD patterns of lindgrenite (black), its triclinic polymorph **4** (red), $CuMo_3O_{10}·H_2O$ (green), MoO_2 (blue) and experimental XRPD pattern (cyan) of sample Cu^{II}: Mo^{VI} = 1:1.25; **c**) green asterisks identify the peaks which correspond to $CuMo_3O_{10}·H_2O$, whereas blue triangle and black squares show the peaks of tugarinovite (MoO_2) and lindgrenite, respectively.

The sample was prepared as follows. A mixture of $Cu(OAc)_2·H_2O$ (480.0 mg, 2.40 mmol, 0.48 M), $(NH_4)_6Mo_7O_{24}·4H_2O$ (530.0 mg, 0.43 mmol, 0.085 M) in 5 mL of water (molar ratio Cu^{II} : Mo^{VI} = 1 : 1.25) was stirred at rt for a few minutes in a 20 mL Teflon-lined autoclave before being sealed. The identical hydrothermal regime to that used for compounds **1-3** was set up. After cooling to rt, a mixture of green powder (lindgrenite), green and dark crystals was isolated. The green species were partially removed using sonication followed by decantation. The residue was filtered off, dried and analyzed.

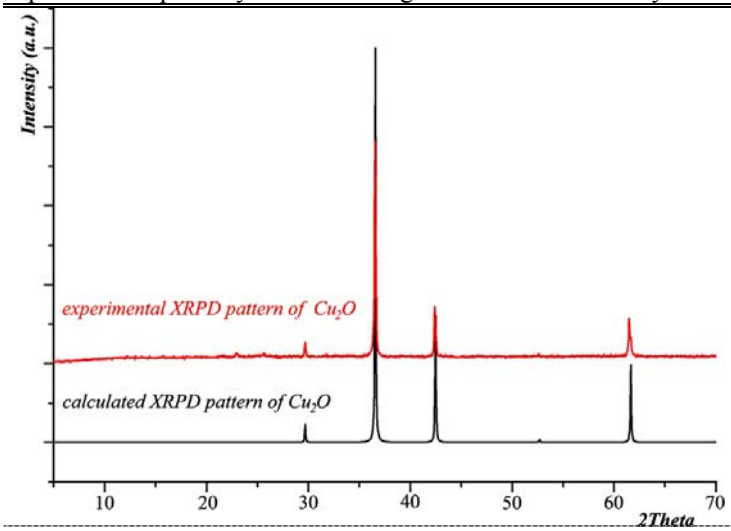

Figure S17. Simulated and experimental XRPD patterns of Cu_2O. The experimental data correspond to the sample prepared under hydrothermal conditions in the reaction between $Cu(OAc)_2·H_2O$ and $(NH_4)_6Mo_7O_{24}·4H_2O$ (Cu^{II}: Mo^{VI} = 8:1).

Table S9. Synthetic conditions and experimental details employed for the construction of the composition-space diagram $Cu(OAc)_2{\cdot}H_2O/tr_2ad/(NH_4)_6Mo_7O_{24}{\cdot}4H_2O$.

Temperature regime: held at 160 °C for 24 h, then cooling to rt for 48 h					
№	Molar ratio Cu^{II}:*tr₂ad*: Mo^{VI}	$Cu(OAc)_2{\cdot}H_2O$ mmol // mg	*tr₂ad* mmol // mg	$(NH_4)_6Mo_7O_{24}{\cdot}4H_2O$ (x 1/7), mmol Mo^{VI} // mg	Reaction products, according XRPD analysis
1	**8:1:1**	0.400// **79.9**	0.050// **13.5**	0.050// **8.8**	complex **3** (major phase) + Cu_2O
2	**7:2:1**	0.350// **69.9**	0.100// **27.0**	0.050// **8.8**	complex **3** (main phase) + Cu_2O
3	**6:3:1**	0.300// **59.9**	0.150// **40.5**	0.050// **8.8**	complex **3** (main phase) + Cu_2O (minor impurity)
4	**5:4:1**	0.250// **49.9**	0.200// **54.0**	0.050// **8.8**	complex **3** (main phase) + Cu_2O (minor impurity)
5	**4:5:1**	0.200// **39.9**	0.250// **67.5**	0.050// **8.8**	complex **2** (main phase) + *tr₂ad* + Cu_2O (minor impurity)
6	**3:6:1**	0.150// **29.9**	0.300// **81.0**	0.050// **8.8**	complex **2** (main phase) + *tr₂ad* + Cu_2O (minor impurity)
7	**2:7:1**	0.100// **20.0**	0.350// **94.5**	0.050// **8.8**	complex **2** (main phase) + *tr₂ad*
8	**1:8:1**	0.050// **10.0**	0.400// **108.0**	0.050// **8.8**	complex **2** + complex **1** + *tr₂ad*
9	**1:7:2**	0.050// **10.0**	0.350// **94.5**	0.100// **17.6**	complex **1** + complex **2** + *tr₂ad*
10	**2:6:2**	0.100// **20.0**	0.300// **81.0**	0.100// **17.6**	complex **2** (main phase) + complex **1** (minor) + *tr₂ad*
11	**3:5:2**	0.150// **29.9**	0.250// **67.5**	0.100// **17.6**	complex **2**
12	**4:4:2**	0.200// **39.9**	0.200// **54.0**	0.100// **17.6**	complex **2**
13	**5:3:2**	0.250// **49.9**	0.150// **40.5**	0.100// **17.6**	complex **2**
14	**6:2:2**	0.300// **59.9**	0.100// **27.0**	0.100// **17.6**	complex **2** (main phase) + Cu_2O (minor impurity)
15	**7:1:2**	0.350// **69.9**	0.050// **13.5**	0.100// **17.6**	complex **2** (main phase) + complex **3** (minor impurity) + unknown phase (trace amount)
16	**6:1:3**	0.300// **59.9**	0.050// **13.5**	0.150// **26.4**	complex **2** (main phase) + complex **3** (minor impurity) + unknown phase (trace amount)
17	**5:2:3**	0.250// **49.9**	0.100// **27.0**	0.150// **26.4**	complex **2**
18	**4:3:3**	0.200// **39.9**	0.150// **40.5**	0.150// **26.4**	complex **2**
19	**3:4:3**	0.150// **29.9**	0.200// **54.0**	0.150// **26.4**	complex **2** (main phase) + complex **1** (minor phase)
20	**2:5:3**	0.100// **20.0**	0.250// **67.5**	0.150// **26.4**	complex **1** (main phase) + complex **2** (minor phase)
21	**1:6:3**	0.050// **10.0**	0.300// **81.0**	0.150// **26.4**	complex **1** (main phase) + complex **2** (minor phase)
22	**1:5:4**	0.050// **10.0**	0.250// **67.5**	0.200// **35.2**	complex **1** (main phase) + *tr₂ad* (impurity)
23	**2:4:4**	0.100// **20.0**	0.200// **54.0**	0.200// **35.2**	complex **1** (main phase) + complex **2** (minor phase)
24	**3:3:4**	0.150// **30.0**	0.150// **40.5**	0.200// **35.2**	complex **1** (main phase) + complex **2** (minor phase)
25	**4:2:4**	0.200// **39.9**	0.100// **27.0**	0.200// **35.2**	complex **2** (main phase) + complex **1** (minor phase)
26	**5:1:4**	0.250// **49.9**	0.050// **13.5**	0.200// **35.2**	complex **2** (main phase) + complex **1** (minor phase)
27	**4:1:5**	0.200// **39.9**	0.050// **13.5**	0.250// **44.0**	complex **1** (main phase) + complex **2** (minor phase)
28	**3:2:5**	0.150// **29.9**	0.100// **27.0**	0.250// **44.0**	complex **1** (main phase) + complex **2** (minor phase)

Table S9. continued

29	**2:3:5**	0.100// **20.0**	0.150// **40.5**	0.250// **44.0**	complex **1** (main phase) + complex **2** (minor phase)
30	**1:4:5**	0.050// **10.0**	0.200// **54.0**	0.250// **44.0**	complex **1**
31	**1:3:6**	0.050// **10.0**	0.150// **40.5**	0.300// **52.8**	complex **1**
32	**2:2:6**	0.100// **20.0**	0.100// **27.0**	0.300// **52.8**	complex **1** (main phase) + complex **2** (minor phase)
33	**3:1:6**	0.150// **29.9**	0.050// **13.5**	0.300// **52.8**	complex **1** (main phase) + complex **2** (minor phase)
34	**2:1:7**	0.100// **20.0**	0.050// **13.5**	0.350// **61.2**	complex **1**
35	**1:2:7**	0.050// **10.0**	0.100// **27.0**	0.350// **61.2**	complex **1**
36	**1:1:8**	0.050// **10.0**	0.050// **13.5**	0.400// **70.4**	complex **1** + impurity of unidentified phase

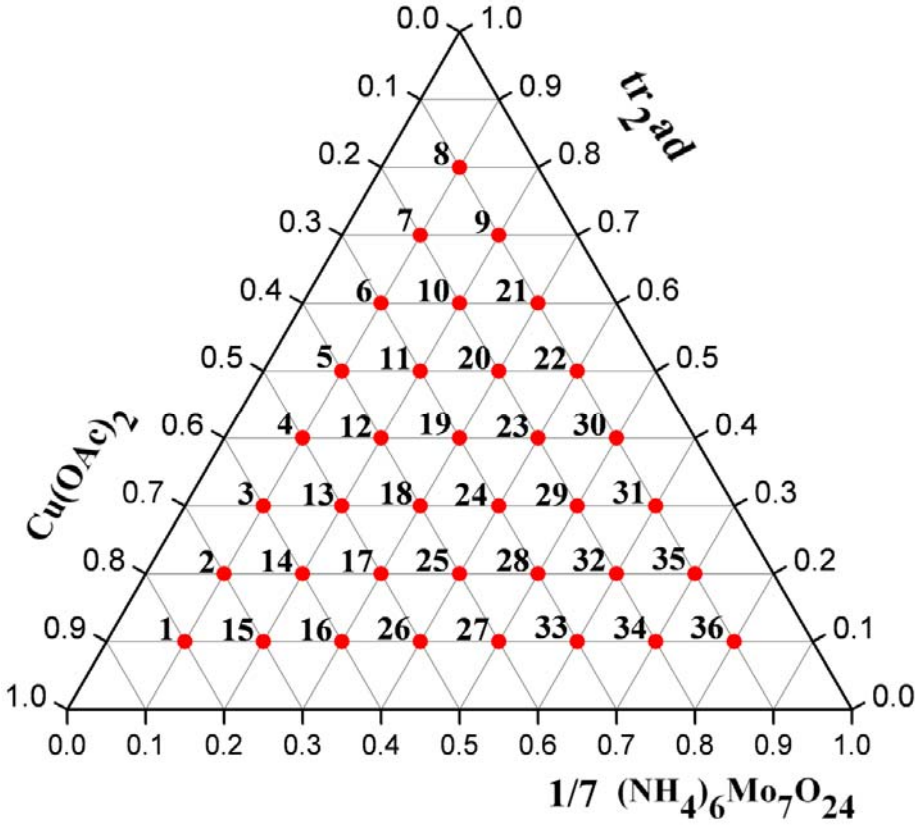

Figure S18. The triangular diagram of $Cu(OAc)_2 \cdot H_2O/tr_2ad/(NH_4)_6Mo_7O_{24} \cdot 4H_2O$ shows 36 reaction points (red) examined in the project.

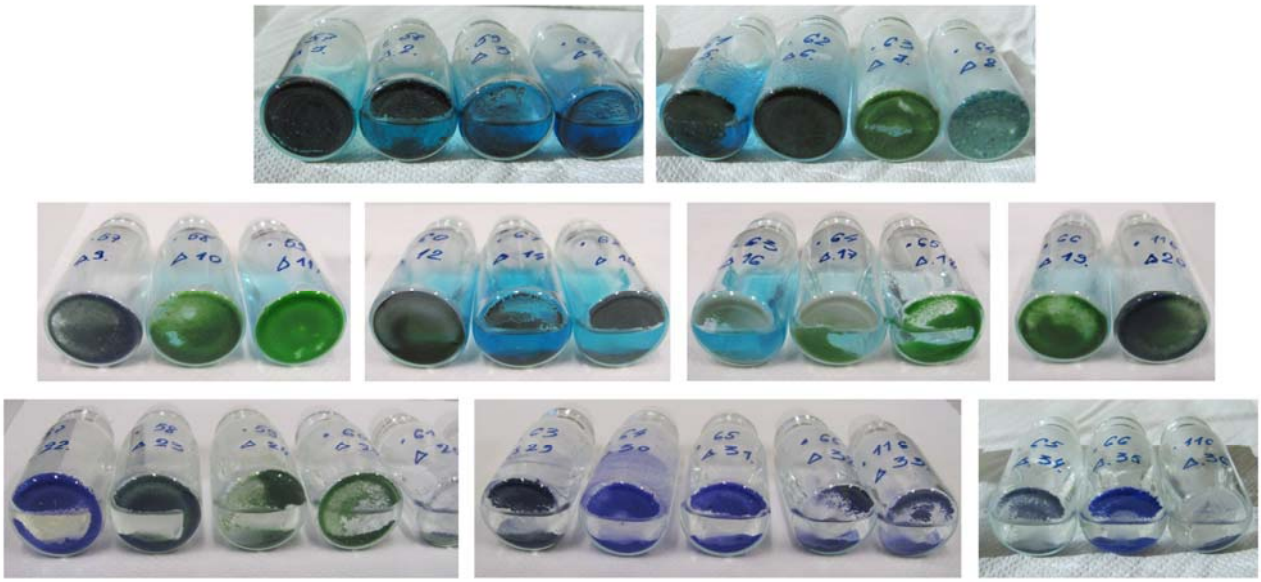

Figure S19. Photographs of reaction products which were isolated and characterized by means of XRPD.

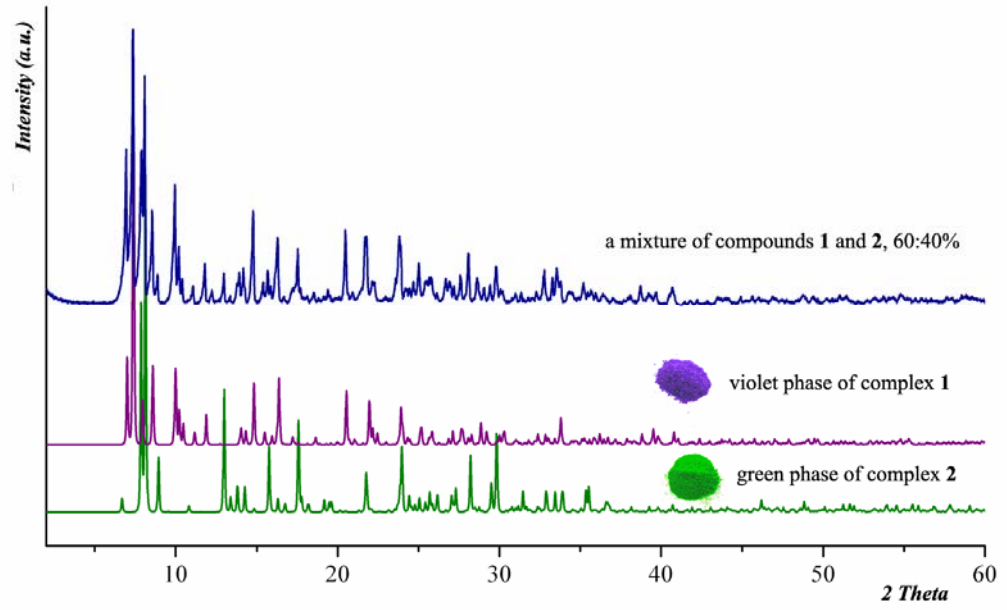

Figure S20. XRPD patterns and photographic images of pure products **1** and **2** and its reaction mixture 60:40%, which was prepared by the hydrothermal reaction between $Cu(OAc)_2$, *tr*$_2$*ad* and $(NH_4)_6Mo_7O_{24}$, with initial reagent ratios of Cu^{II}: *tr*$_2$*ad*: Mo^{VI}= 3 : 2: 5.

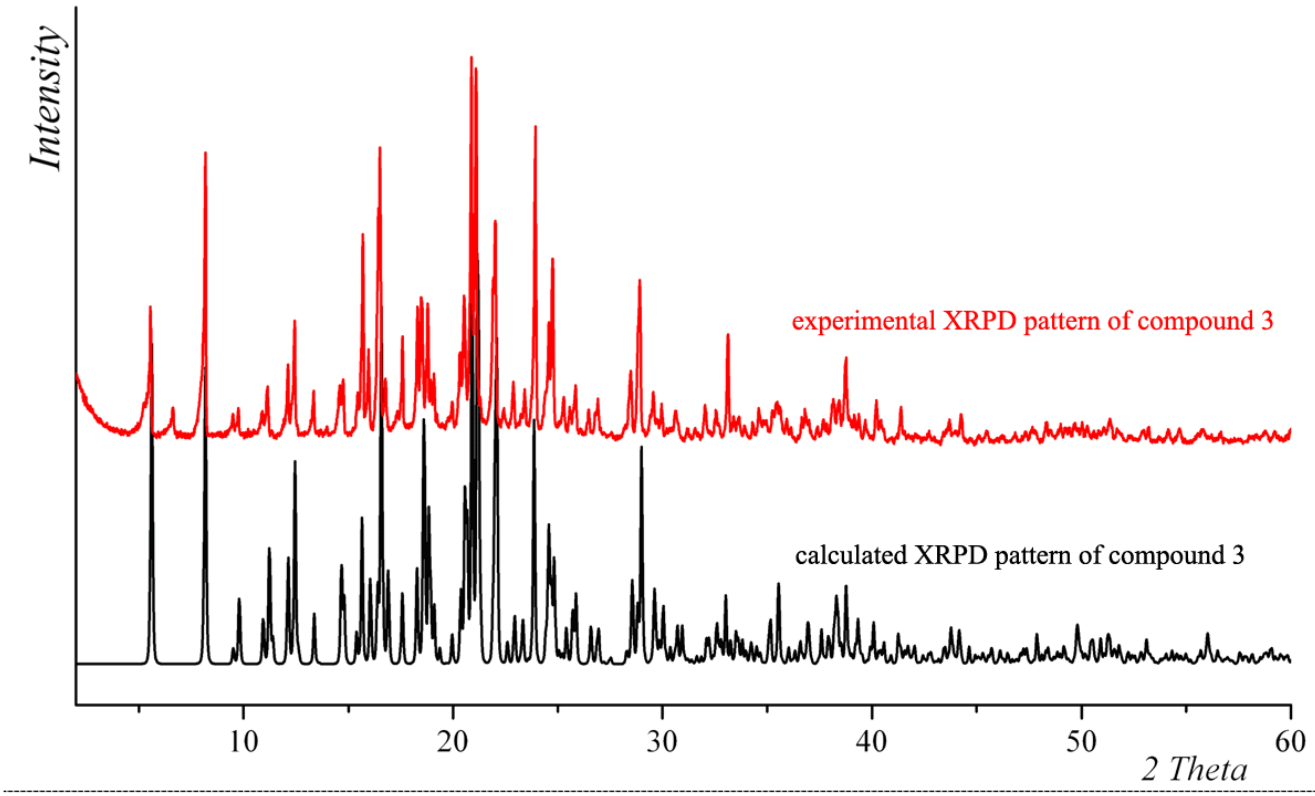

Figure S21. XRPD patterns (simulated and experimental) of complex **3**.

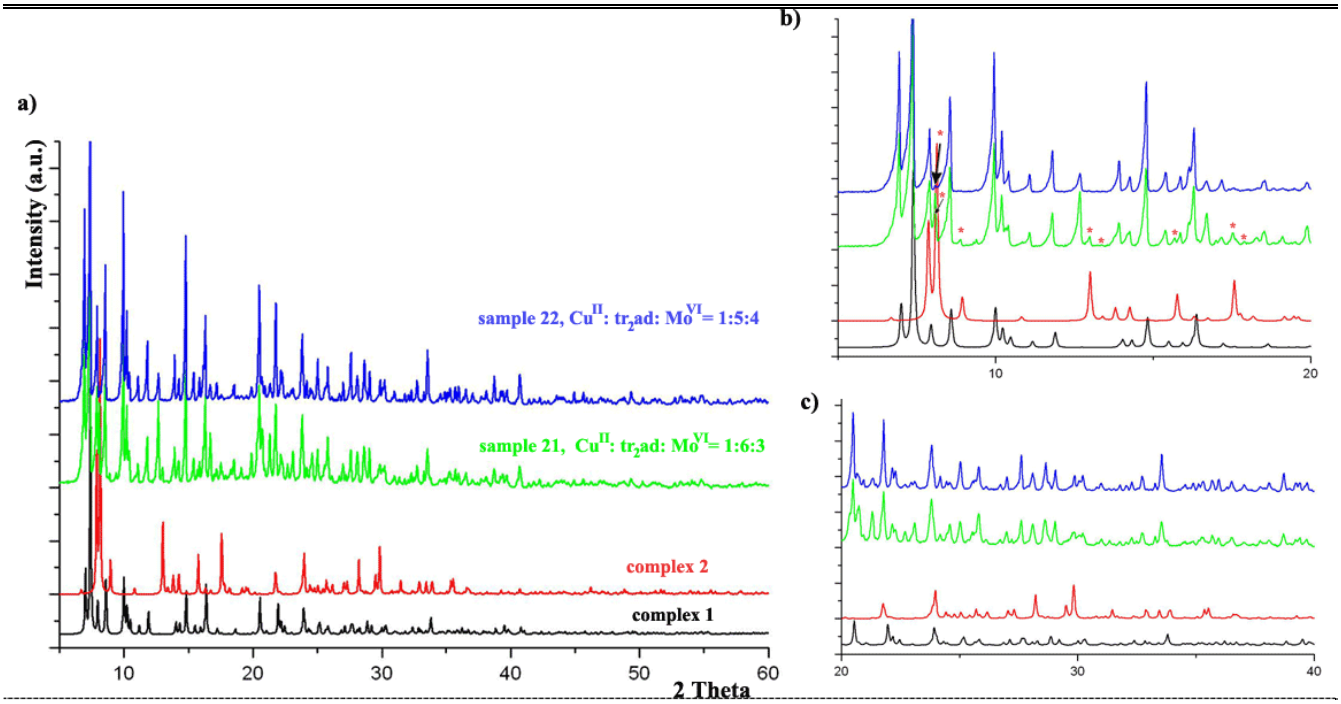

Figure S22. **a)**, **b)**, **c)**. Simulated XRPD patterns of complexes **1** (black) and **2** (red) as well as experimental XRPD data of samples **21** (green - Cu^{II}: *tr*$_2$*ad*: Mo^{VI} = 1:6:3) and **22** (blue - Cu^{II}: *tr*$_2$*ad*: Mo^{VI} = 1:5:4) (see also Table S10). The experimental patterns confirm the presence of **1** (main phase) and **2** (minor phase identified by red asterisks) in the reaction mixture.

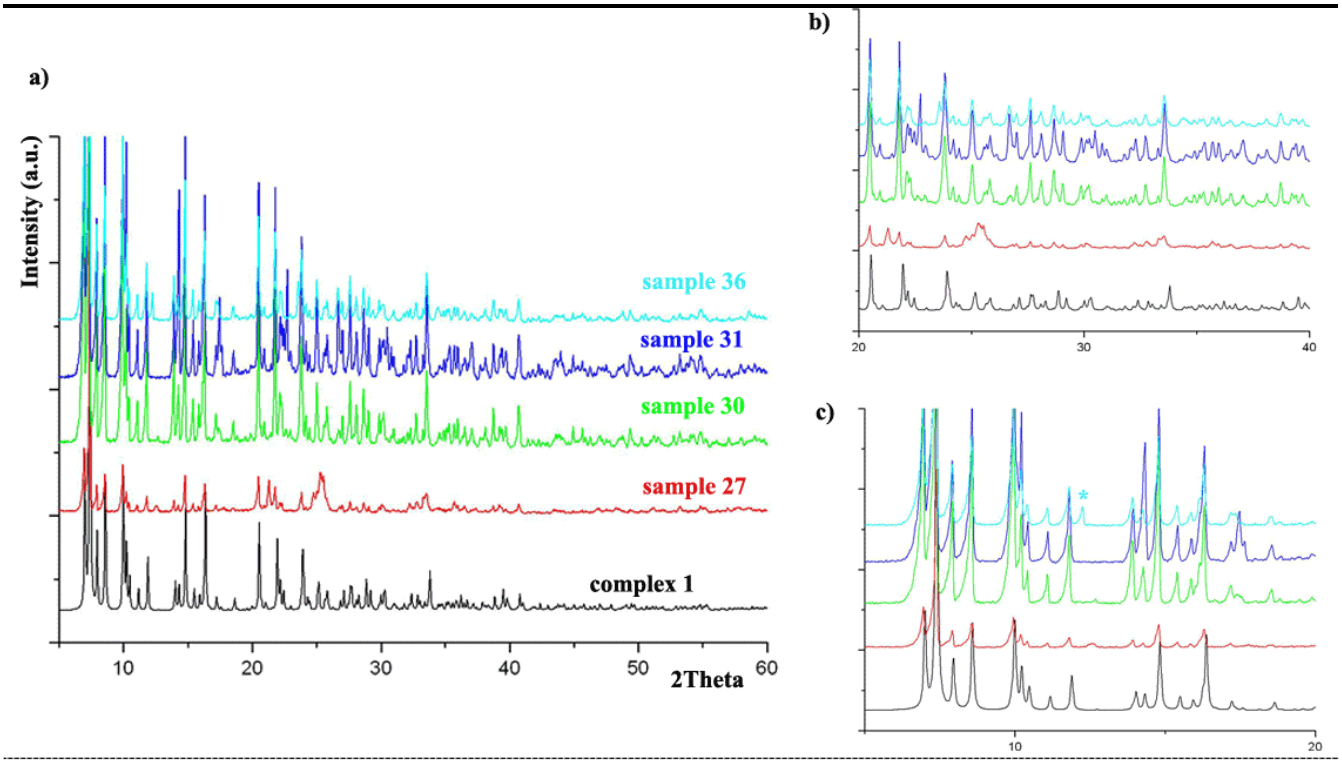

Figure S23. **a)**, **b)**, **c)**. Simulated XRPD pattern of complex **1** and experimental XRPD data of samples **27** (red - Cu^{II}: tr_2ad: Mo^{VI} = 4:1:5) and **30** (green - Cu^{II}: tr_2ad: Mo^{VI} = 1:4:5), **31** (blue - Cu^{II}: *tr₂ad*: Mo^{VI} = 1:3:6) and **36** (cyan - Cu^{II}: *tr₂ad*: Mo^{VI} = 1:1:8). These data demonstrate that compound **1** dominates in the reaction mixture; **c)** asterisk indicates the presence of an unidentified phase.

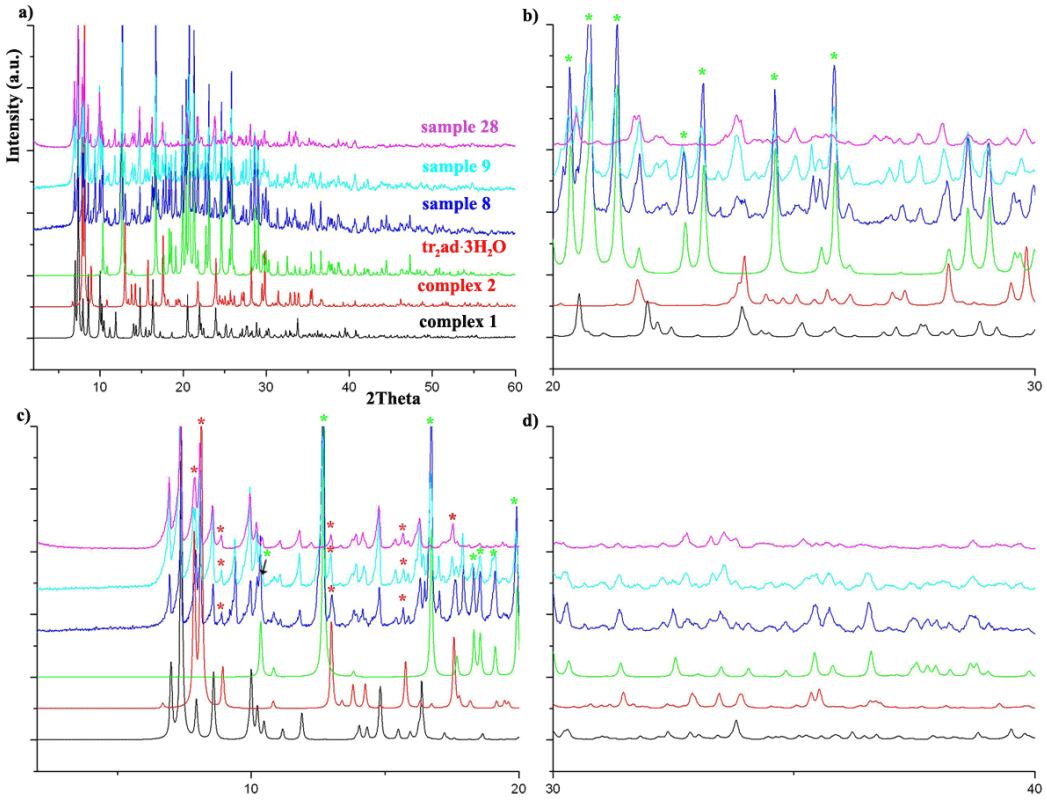

Figure S24. **a)**, **b)**, **c)** and **d)**. Simulated XRPD patterns of compounds **1** (black), **2** (red) and $tr_2ad{\cdot}3H_2O$ (green) as well as experimental XRPD data of samples **8** (blue - Cu^{II}: tr_2ad: Mo^{VI} = 1:8:1), **9** (cyan - Cu^{II}: *tr₂ad*: Mo^{VI} = 1:7:2) and **28** (magenta - Cu^{II}: *tr₂ad*: Mo^{VI} = 3:2:5). According to the results; the reaction mixtures consist of complexes **1** and **2** (sample 28) or **1**, **2** and $tr_2ad{\cdot}3H_2O$ (samples 8, 9); **b)**, **c)** Red and green asterisks indicate the presence of complex **2** and $tr_2ad{\cdot}3H_2O$, respectively (see also details in Table S10).

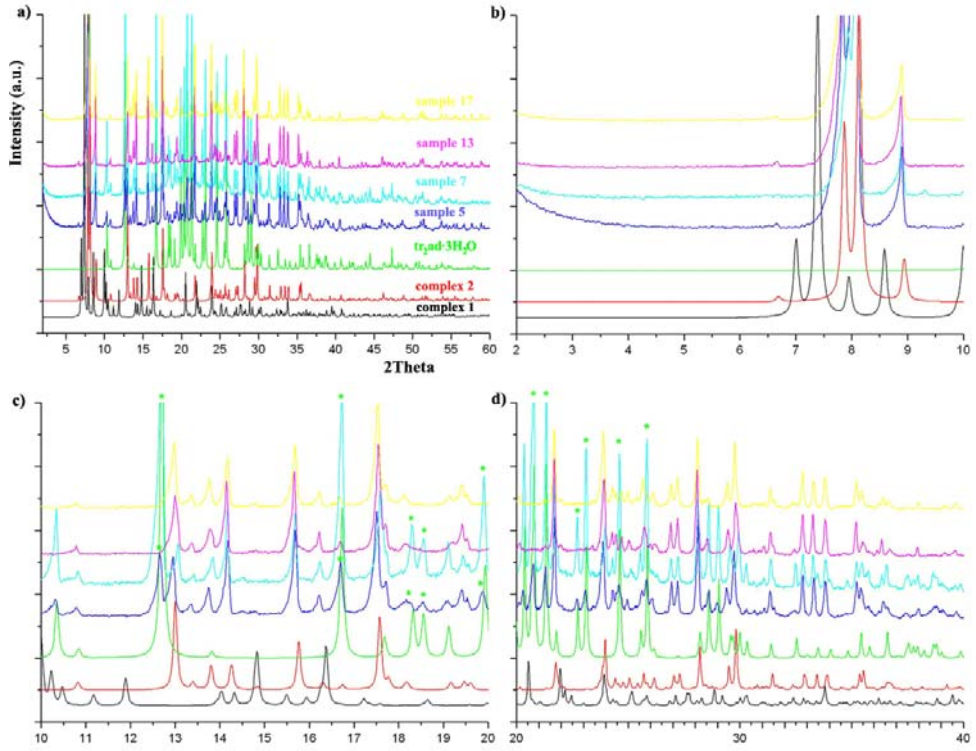

Figure S25. **a)**, **b)**, **c)** and **d)**. Simulated XRPD patterns of compounds **1** (black), **2** (red) and $tr_2ad{\cdot}3H_2O$ (green) as well as experimental XRPD data of samples 5 (blue - Cu^{II}: *tr₂ad*: Mo^{VI} = 4:5:1), 7 (cyan - Cu^{II}: *tr₂ad*: Mo^{VI} = 2:7:1), 13 (magenta - Cu^{II}: *tr₂ad*: Mo^{VI} = 5:3:2) and 17 (yellow - Cu^{II}: *tr₂ad*: Mo^{VI} = 5:2:3). According to the results, samples 5 and 7 consist of a mixture of complex **2** and $tr_2ad{\cdot}3H_2O$, whereas samples 13, 17 can be identified as complex **2**; **c)**, **d)** green asterisks indicate the presence of $tr_2ad{\cdot}3H_2O$.

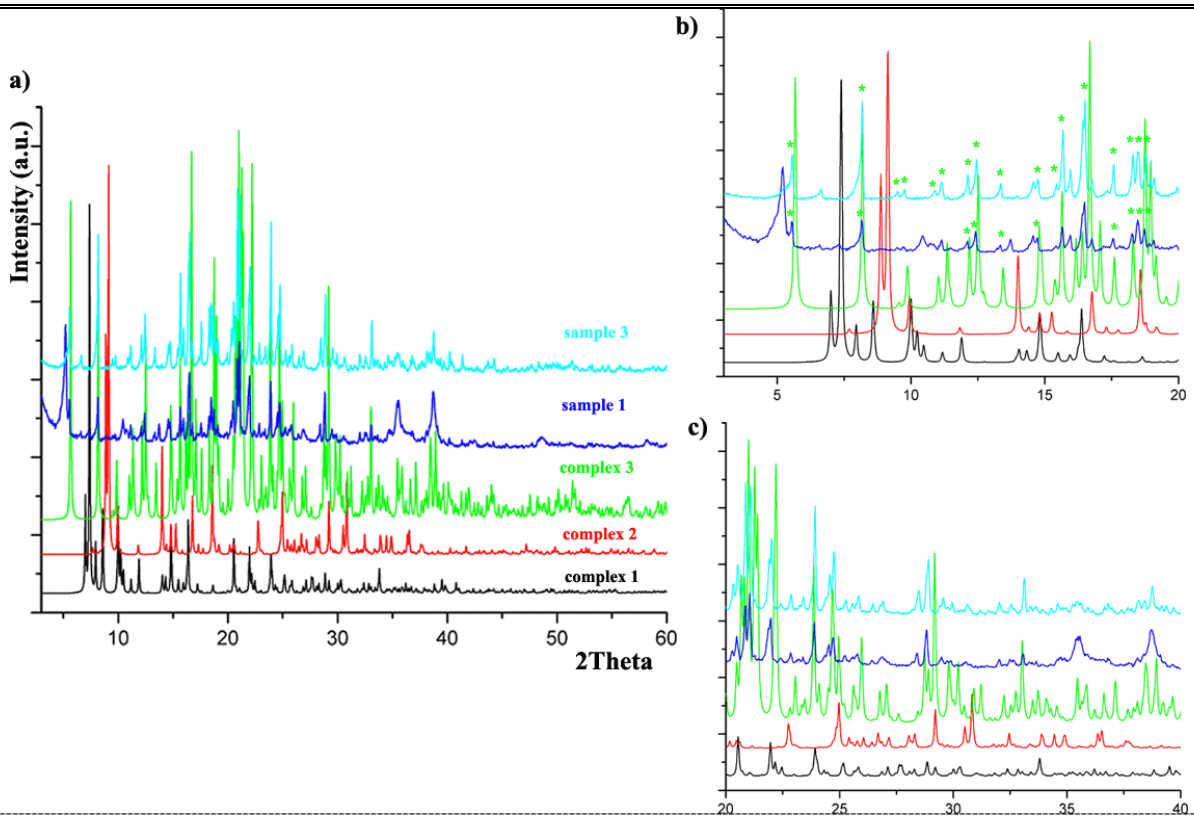

Figure S26. **a)**, **b)** and **c)**. Simulated XRPD patterns of compounds **1** (black), **2** (red) and **3** (green) as well as experimental XRPD data of samples **1** (blue - Cu^{II}: *tr₂ad*: Mo^{VI} = 8:1:1) and **3** (cyan - Cu^{II}: *tr₂ad*: Mo^{VI} = 6:3:1); **b)** green asterisks indicate the presence of complex **3** as main crystalline phase.

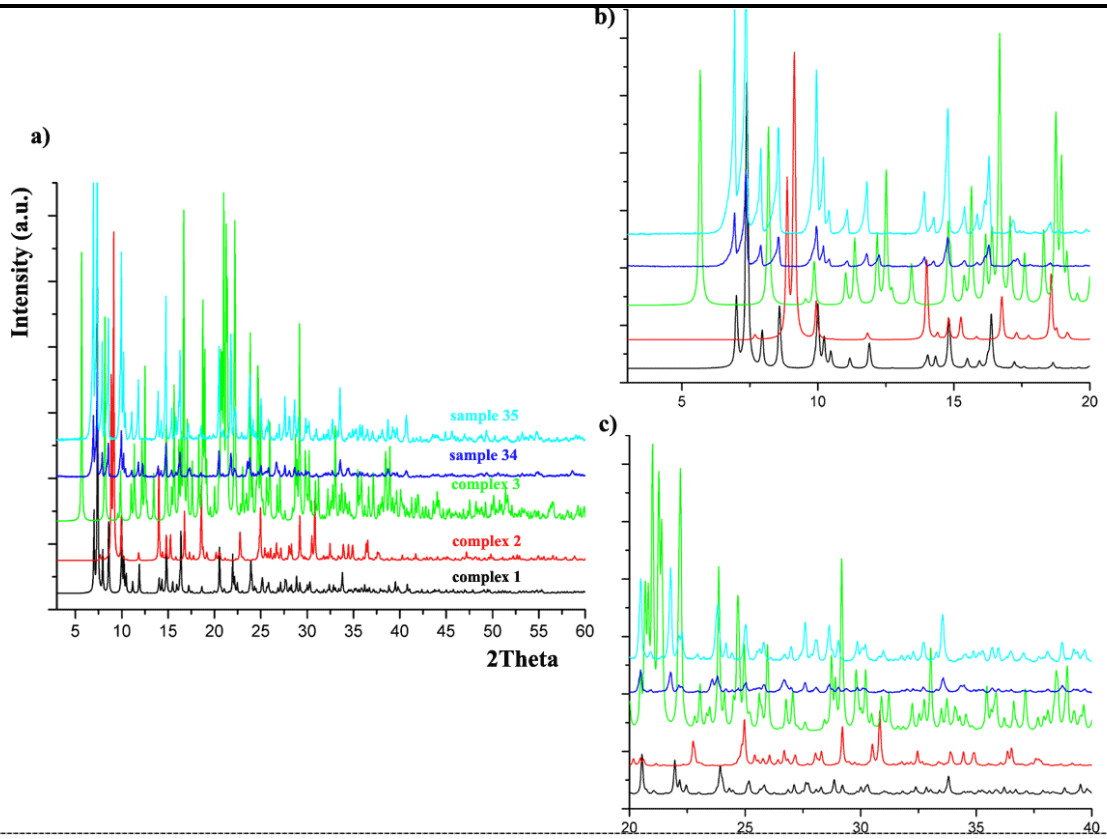

Figure S27. **a)**, **b)** and **c)**. Simulated XRPD patterns of complexes **1** (black), **2** (red) and **3** (green) as well as experimental XRPD data of samples **34** (blue - Cu^{II}: *tr*$_2$*ad*: Mo^{VI} = 2:1:7) and **35** (cyan - Cu^{II}: *tr*$_2$*ad*: Mo^{VI} = 1:2:7). These data confirm the bulk-phase purity of complex **1**.

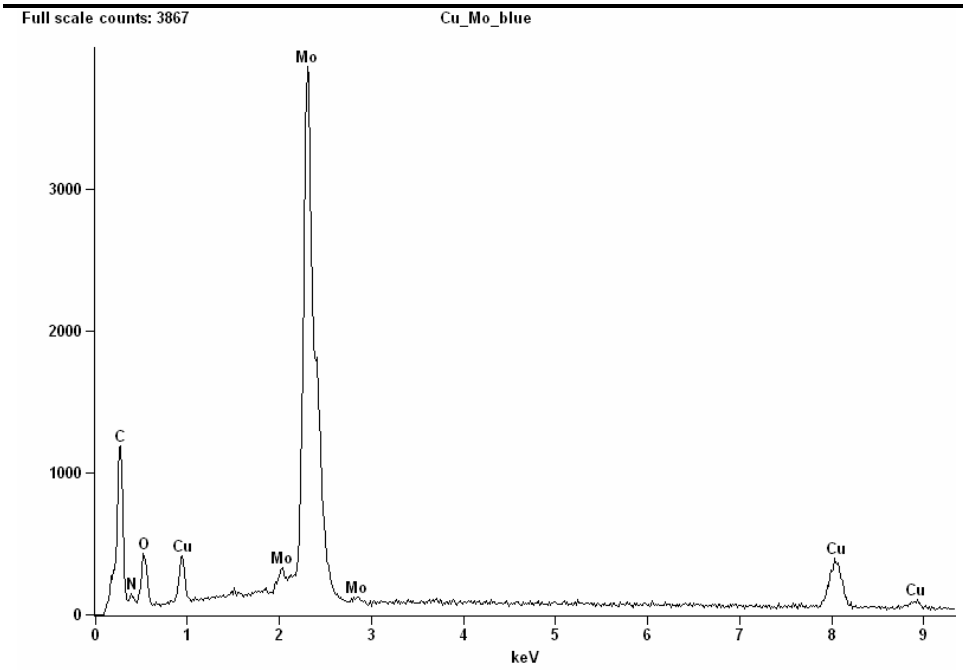

Live Time: 100.0 sec. Acc. Voltage: 25.0 kV Take Off Angle: 35.2 deg.

Cu_Mo_blue(1)

Element Line	*Weight %*	*Weight % Error*	*Atom %*	*Atom % Error*
Cu K	13.76	+/- 0.56	19.42	+/- 0.79
Mo L	86.24	+/- 0.99	80.58	+/- 0.92
Total	100.00		100.00	

Figure S28. EDS spectrum of compound **1**.

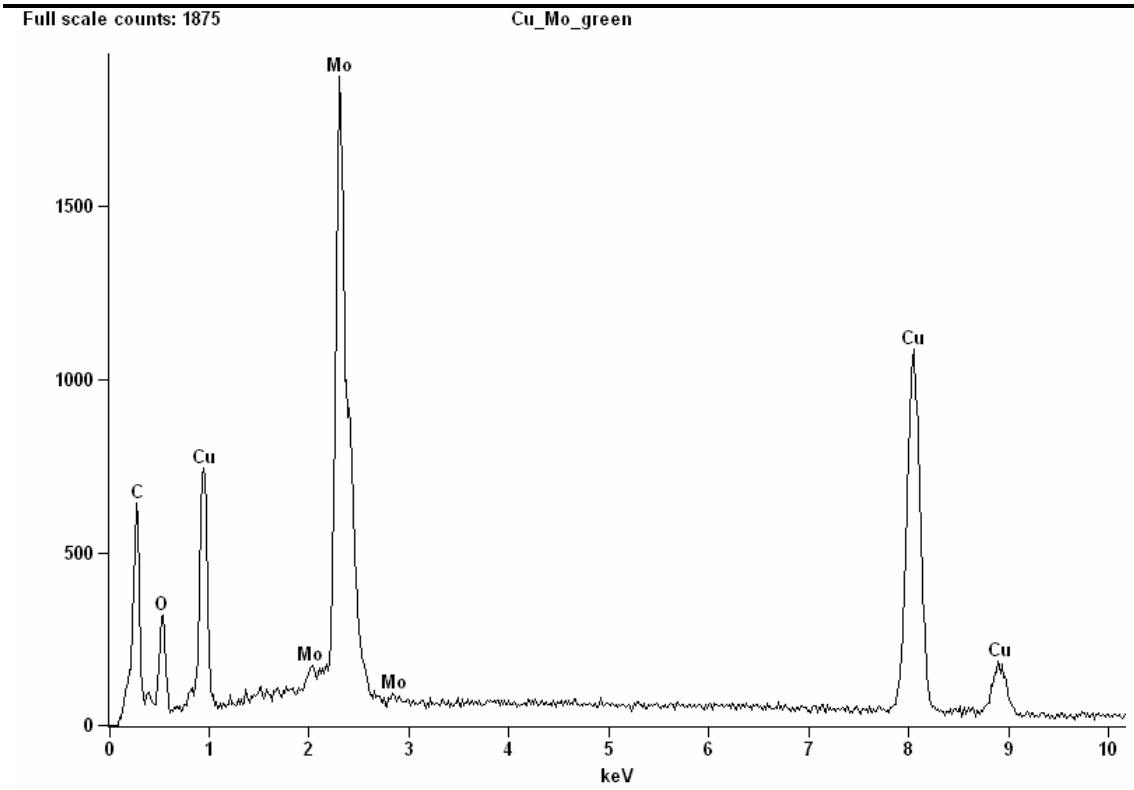

Live Time: 100.0 sec. Acc. Voltage: 25.0 kV Take Off Angle: 35.2 deg.

Cu_Mo_green(1)

Element Line	*Weight %*	*Weight % Error*	*Atom %*	*Atom % Error*
Cu K	45.88	+/- 0.82	56.14	+/- 1.00
Mo L	54.12	+/- 1.02	43.86	+/- 0.83
Total	100.00		100.00	

Figure S29. EDS spectrum of compound **2**.

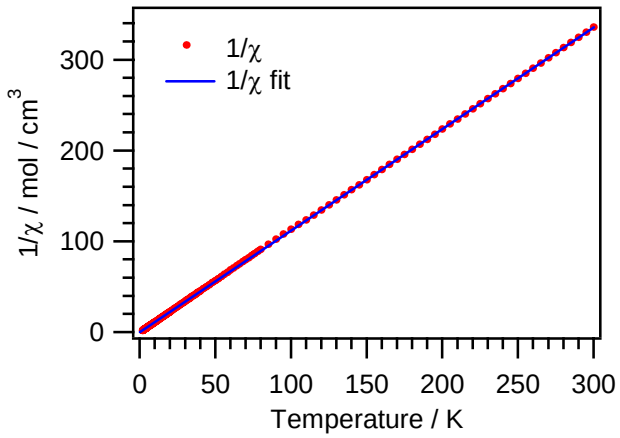

Figure S30. Inverse magnetic susceptibility *vs* temperature for **1** (solid line represents a Curie-Weiss fit in the temperature range 150–300 K).

References:

S1. (a) Stoe & Cie. X-SHAPE. Revision 1.06, Stoe & Cie GmbH, Darmstadt, Germany, **1999**; (b) Stoe & Cie. X-RED. Version 1.22, Stoe & Cie GmbH, Darmstadt, Germany, **2001**.

S2. (a) Sheldrick, G. M. *Acta Crystallogr*. **1990**, *A46*, 467. (b) Sheldrick, G. M. *Acta Crystallogr.* **2008**, *A64*, 112.

S3. Brandenburg, K. Diamond 2.1e, Crystal Impact GbR, Bonn, **1999**.

S4. For C--H...Acceptor Interactions See: Steiner, Th. *Cryst. Rev*, **1996**, *6*, 1-57.

S5. Jeffrey, G. A.; Maluszynska, H.; Mitra, J. *Int.J.Biol.Macromol*. **1985**, *7*, 336-348.